

DOCUMENT RESUME

ED 114 124

IR 002 761

AUTHOR Larson, D. F.; Terry, C.
 TITLE Advanced Simulation in Undergraduate Pilot Training: Systems Integration. Final Report (February 1972-March 1975).
 INSTITUTION Air Force Human Resources Lab., Brooks AFB, Texas.
 REPORT NO AFHRL-TR-75-59(7)
 PUB DATE Oct 75
 NOTE 69p.

EDRS PRICE MF-\$0.76 HC-\$3.32 Plus Postage
 DESCRIPTORS Aircraft Pilots; Autoinstructional Programs; Computer Assisted Instruction; Educational Programs; *Flight Training; *Instructional Systems; Integrated Activities; Military Training; *Simulators; Training Techniques; *Undergraduate Study

IDENTIFIERS *Advanced Simulator Undergraduate Pilot Training; ASUPT; CIG; Computer Image Generator; ICD; Interface Control Document

ABSTRACT

The Advanced Simulator for Undergraduate Pilot Training (ASUPT) was designed to investigate the role of simulation in the future Undergraduate Pilot Training (UPT) program. The problem addressed in this report was one of integrating two unlike components into one synchronized system. These two components were the Basic T-37 Simulators and their various subcomponents developed by Singer under another contract, and the Computer Image Generator (CIG), developed by General Electric. This integration included not only the physical mating of the CIG system with the basic simulator computer, instructor-operator stations, visual displays, and cockpits, but also the computer software integration to make the visual scene correlate with the flight instruments and the real world. The selected approach to integrating the CIG system was one of planned organization. An Interface Control Document (ICD) was drafted early in the program which identified the hardware and the software interface between the two systems. The authors concluded that the success of this effort was in the organization and maintenance of the ICD and the advance planning for the integration of the computer systems. (Author/HB)

 * Documents acquired by ERIC include many informal unpublished, *
 * materials not available from other sources. ERIC makes every effort *
 * to obtain the best copy available. Nevertheless, items of marginal *
 * reproducibility are often encountered and this affects the quality *
 * of the microfiche and hardcopy reproductions ERIC makes available *
 * via the ERIC Document Reproduction Service (EDRS). EDRS is not *
 * responsible for the quality of the original document. Reproductions *
 * supplied by EDRS are the best that can be made from the original. *

AIR FORCE



HUMAN RESOURCES

**ADVANCED SIMULATION IN
UNDERGRADUATE PILOT TRAINING:
SYSTEMS INTEGRATION**

SCOPE OF INTEREST NOTICE

The ERJC Facility has assigned
this document for processing
to:

IR

CE

In our judgement, this document
is also of interest to the clearing-
houses noted to the right. Index-
ing should reflect their special
points of view.

By

D. F. Larson

C. Terry

Singer-Simulation Products Division
Binghamton, New York 43902

ADVANCED SYSTEMS DIVISION
Wright-Patterson Air Force Base, Ohio 45433

October 1975

Final Report for Period February 1972 - March 1975

Approved for public release; distribution unlimited.

LABORATORY

AIR FORCE SYSTEMS COMMAND
BROOKS AIR FORCE BASE, TEXAS 78235

ED114124

U.S. DEPARTMENT OF HEALTH,
EDUCATION & WELFARE
NATIONAL INSTITUTE OF
EDUCATION

THIS DOCUMENT HAS BEEN REPRO-
DUCED EXACTLY AS RECEIVED FROM
THE PERSON OR ORGANIZATION ORIGIN-
ATING IT. POINTS OF VIEW OR OPINIONS
STATED DO NOT NECESSARILY REPRE-
SENT OFFICIAL NATIONAL INSTITUTE OF
EDUCATION POSITION OR POLICY

200 2 761



NOTICE

When US Government drawings, specifications, or other data are used for any purpose other than a definitely related Government procurement operation, the Government thereby incurs no responsibility nor any obligation whatsoever, and the fact that the Government may have formulated, furnished, or in any way supplied the said drawings, specifications, or other data is not to be regarded by implication or otherwise, as in any manner licensing the holder or any other person or corporation, or conveying any rights or permission to manufacture, use, or sell any patented invention that may in any way be related thereto.

This final report was submitted by Singer-Simulation Products Division, Binghamton, New York 13902, under contract F33615-72-C-1557, project 1192, with Advanced Systems Division, Air Force Human Resources Laboratory (AFSC), Wright-Patterson Air Force Base, Ohio 45433. Mr. William B. Albery, Simulation Techniques Branch, was the contract monitor.

This report has been reviewed and cleared for open publication and/or public release by the appropriate Office of Information (OI) in accordance with AFR 190-17 and DoDD 5230.9. There is no objection to unlimited distribution of this report to the public at large, or by DDC to the National Technical Information Service (NTIS).

This technical report has been reviewed and is approved.

GORDON A. ECKSTRAND, Director
Advanced Systems Division

Approved for publication.

HAROLD E. FISCHER, Colonel, USAF
Commander

SUMMARY

PROBLEM

The Advanced Simulator for Undergraduate Pilot Training (ASUPT) is a research device designed for investigating the role of simulation in the future Undergraduate Pilot Training (UPT) program. For ASUPT to be effective in training research, it must faithfully simulate all aspects of flight. This includes not only the extra-cockpit visual cues, but also the motion and forces exerted on the pilot by the simulator, and all of the sights and sounds to which he is accustomed. This report describes the integration of these sights, sounds, and motions into a coordinated, composite system - ASUPT.

The problem addressed in this report is one of integrating two unlike components into one synchronized system. These two components are the Basic T-37 Simulators and their various subcomponents developed by Singer under another contract and the Computer Image Generator, or CIG, developed by General Electric. This integration included not only the physical mating of the CIG system with the basic simulator computer, instructor-operator stations, visual displays, and cockpits, but also the computer software integration to make the visual scene correlate with the flight instruments and the real world. The problem represented the first of its kind in that it was the first full digital visual system to be integrated with a state-of-the-art, high fidelity flight simulator.

APPROACH

The selected approach to integrating the Basic Simulators and the CIG systems was one of planned organization. An Interface Control Document ICD was drafted early in the program which identified the hardware and software interface between the two systems. The goal of the ICD was for each responsible contractor to identify and quantify each interface parameter well in advance of the actual integration. Various working meetings were held among the Contractors and the Air Force and plans for installation, cabling, computer integration, and testing were established and agreed upon. After the computers were updated and integrated, the major problem then was one of changing the flight model in order to correct for deficiencies not detectable without a visual system.

RESULTS

The integration was begun in early October 1974 with the mating of the Basic Simulators and CIG general purpose computers. After this was

accomplished, the test guide was trial run through November 1974. Formal testing of the interface began in December 1974 and the fully integrated ASUPT was accepted by the Air Force 17 Jan 75.

CONCLUSIONS

This effort represents the first of its kind in simulation; the mating of a fully digital visual system with an advanced flight simulator. The success of this effort lies in the organization and maintenance of an Interface Control Document and the advance planning for the integration of the computer systems.

PREFACE

This report is the 7th of seven volumes describing the Advanced Simulation in Undergraduate Pilot Training (ASUPT) system development program. The seven volumes of AFHRL-TR-75-59 are as follows:

Volume I: Advanced Simulation in Undergraduate Pilot Training:
An Overview

Volume II: Advanced Simulation in Undergraduate Pilot Training:
Motion System Development

Volume III: Advanced Simulation in Undergraduate Pilot Training:
G-Seat Development

Volume IV: Advanced Simulation in Undergraduate Pilot Training:
Automatic Instructional System

Volume V: Advanced Simulation in Undergraduate Pilot Training:
Computer Image Generation

Volume VI: Advanced Simulation in Undergraduate Pilot Training:
Visual Display Development

Volume VII: Advanced Simulation in Undergraduate Pilot Training:
Systems Integration

This project derived from a DOD Directive to the three Services requesting programs of advanced development in the area of training and education. The purpose was to insure that military training and education make the fullest use of recent innovations and technological advances. In October 1967, a joint Air Training Command/Air Force Human Resources Laboratory effort culminated in a recommendation to establish an advanced simulation system at an undergraduate pilot training base. Hardware development of the ASUPT began in 1971 and the system was released for research in Jan 75.

All members of the ASUPT Program Office and participating organizations who worked on the program contributed to the final system. In addition to the listed contract monitors, they include Don Gum, ASUPT Program Manager, James Basinger, CIG Project Engineer, Israel Guterman, Basic Simulators Project Engineer, William Albery, Systems Integration Project Engineer, Patricia Knoop, Advanced Training Systems Project Engineer, Kenneth Block, Program Controller, and Virginia Lewis, Secretary, all of the Advanced Systems Division, Air Force Human Resources Laboratory, Wright-Patterson AFB OH; Warren Richeson, Capt Frank Bell III, Maj Ray Fuller, Capt John Fuller, Capt Dennis Way, Capt Steve Rust, Capt Mike Cyrus, and Mr. Glenn York, all from the Flying Training Division, Air Force Human Resources Laboratory, Williams AFB AZ.

TABLE OF CONTENTS

	Page
Introduction	5
Optimization	7
Visual Interface	8
Modules	8
Simulator/CIG Interface Data	9
CIG/Simulator Synchronization	14
Transport Delay	16
Time Compensation	17
Cue Correction	21
Flight	22
Attitude Control	22
Ground Control	25
Spins	33
Formation Flight	41
Record/Playback (R/P)	43
Summary	45
References	46
Appendix A - ASUPT Technical Fact Sheet	47

LIST OF ILLUSTRATIONS

Figure		Page
1	Worst Case Visual Transport Delay	10
2	Flight/Nav and Display Timing	17
3	Aileron Force vs. Control Stick Position	24
4	Aileron Deflection vs. Control Position	24
5	Main Tire Cornering Power vs. Main Strut Vertical Force	30
6	Nose Tire Cornering Power vs. Nose Strut Vertical Force	31
7	Basic Pitch Coefficient vs. Angle of Attack	40

LIST OF TABLES

Table		Page
1	Simulator to CIG Arithmetic Data Transfers for A, B, and Lead Blocks	11
2	Simulator to CIG Discrete Data Transfers for A, B, and Lead Blocks	12
3	CIG to Simulator Discrete Data Transfers for Cockpits A and B	13

INTRODUCTION

The ASUPT simulator/CIG integration effort is the first of its kind in the respect that it is the first full digital visual system (terrain and T-37 model) to be integrated with an operational flight trainer. This report describes the problems and solutions associated with the accomplishment of this task. As one may expect, some problems are common with model visual systems such as ground reactions. Accordingly, other problems are unique to a digital system, such as timing and iteration rates.

The ASUPT facility (located at Williams AFB, Arizona) consists of three primary systems (see Appendix A for a description of the ASUPT system):

- (1) Simulators
- (2) Visual System Displays
- (3) Computer Image Generator (CIG)

The simulators and visual system displays were procured by the Air Force under contract to Singer-SPD in 1971. Delivery of the systems was made to WAFB, in the fall of 1973, with final acceptance by AFHRL in February of 1974.

The computer image generator (CIG) system was procured by the Air Force from the General Electric Company in 1972, and was delivered and accepted at WAFB in September 1974.

In 1971, Singer-SPD contracted to integrate the simulator and CIG systems. Actual integration began with the procurement of the CIG and was regulated and controlled by an SPD-generated Interface Control Document (ASUPT-59)² monitored by AFHRL. Computer integration began in October of 1974 and was followed by the ASUPT/CIG integration which was completed 17 January 1975.

Prior to the final integration phase, the following integration-related events were completed:

- (1) Simulator visual interface subroutine development and stand-alone debug.
- (2) Integration of the visual interface programs with the simulator real-time load.
- (3) Physical mounting, cabling, and alignment of CRT tubes, electronics, instructor station monitors, etc.
- (4) Testing and verification of the simulator and CIG systems in an independent but concurrent mode.

(5) Testing and verification of the visual display system hardware and CRT electronics integrity during platform motion.

The final integration phase consisted of the following major events:

(1) Computer integration (CIG computer complex and simulator complex).

(2) Basic simulator systems tailoring.

(3) Total integrated system acceptance testing.

Computer integration consisted of the following events:

(1) Cabling the last 8K words of the simulator computer to the CIG general-purpose computer to allow interfacing of data between the two systems.

(2) Cabling a common CPU, memory, and automatic input/output system clock source for the two CIG and one simulator general-purpose (GP) computers.

(3) Bringing all three GP's up to the latest ECO level. This task was performed by Systems Engineering Laboratories (SEL) under subcontract to Singer-SPD.

The remaining two events, basic simulator systems tailoring and total integrated system acceptance testing, began concurrent with the SEL activity and were successfully completed in January 1975. The test guide and results are documented in ASUPT-76.¹ The major problems anticipated or encountered during this final integration, along with their solutions, are the subject of this report. Problems related to the CIG system itself are not documented in this report.

Because of the demands of AFHRL in requiring a well-maintained Interface Control Document (ICD)² as a vehicle for information exchange between Singer-SPD and General Electric, preliminary integration problems (e.g., CIG assemblies mounting in the cockpit and instructor stations) were minimal when final integration began. Consequently, the major integration effort consisted of upgrading or tailoring the basic simulator systems to meet the increased fidelity required from the simulated aircraft dynamics which manifested themselves in the visual cues. In addition, modification was necessary to correlate the simulator navigation data bases with the CIG to ensure correspondence between the CIG environment and simulator displays, such as cross-country track and GCA approaches. Addition of the visual, and resulting modifications to simulator dynamics, also increased timing overhead on the simulator computer, resulting in the need to optimize the simulator load to ensure high fidelity simulation during worst-case system configurations and to meet

the background (core and time) requirements of the statement of work (SOW).

Although the basic simulator dynamics were designed from the beginning to meet resolution requirements for a smooth visual display, certain problems could only be anticipated and planned for; their solution had to be addressed during the course of actual integration when the problem could be seen.

OPTIMIZATION

In order to meet SOW specifications for spare core and time, and to accommodate the increased core and time demanded by inclusion of the visual interface modules and upgrading of the simulator dynamics, existing modules required optimization. Without optimization, successful integration was not possible. The simulator was capable of handling an average configuration of both cockpits active with motion, G-seat, and visual; however, placing one cockpit in a formation flying mode overloaded every other frame. The executive, although designed to distribute one frame's excess into another's spare, could not catch up. Simulation fidelity degraded, operator software-driven displays failed, and training was impossible until one cockpit was placed off-line. Likewise, it was determined that two modules, one computing formation flying inertial axis separation and the other computing aircraft position, would have to be increased from a 7.5/second to a 15/second iteration rate to eliminate objectionable translational stepping and resulting pilot control problems during formation flying. Examination of timing statistics showed that approximately 10 to 15 milliseconds per frame were needed to fit the load in the 66.67-millisecond frame and meet spare time requirements of 20 percent. Initial optimization efforts began immediately upon final integration and continued throughout the integration phase. These efforts consisted primarily of the following:

(1) Optimization of assembler and Fortran techniques, e.g., replacing square and divide functions with multiply functions.

(2) Reducing the formation flying wake and downwash model to compute dynamic effects on two lag aircraft wing points rather than four.

(3) Modification of the linear function interpolator (LFI) jump list to allow slow computed functions to be called at rates of 7.5/second rather than 15/second.

(4) Implementing faster methods for calling operating system services.

(5) Optimizing instrument drive programs to eliminate unnecessary Fortran conversion calls.

(6) Eliminating built-in but virtually unused test functions from the motion, G-seat, and navigation system modules.

(7) Disabling unnecessary interrupts.

(8) Restructuring the module jump list to provide better load distribution and symmetry.

Significant results were achieved, resulting in a core increase of approximately 8K words and time of approximately 12 milliseconds/frame. The success of this effort resulted in the elimination of numerous problems manifested in all systems, not just the visual system, and allowed full configuration use of the simulator, including the capability to perform batch operations in the spare frame or background time.

VISUAL INTERFACE

Modules

Three modules were developed to perform the functions necessary to interface the basic simulator with the CIG, and they are:

(1) Visual Fast subroutine

(2) Visual Slow subroutine

(3) Visual Logic subroutine

The Visual Slow subroutine is called once per second by the simulator executive. It computes the sines and cosines of the angular corrections necessary to correct the flight system's flat-earth heading to map heading. This correction contains both the transport angle and the meridian convergence. The transport angle is employed by the simulator navigation programs as well as the Visual Slow subroutine to transform flight heading to spherical earth (true) heading. The meridian convergence correction is necessary to compensate for the transverse Mercator mapping scheme, to which the CIG environment data base is modeled.

The Visual Logic subroutine is called 3.75 times per second by the simulator executive. It performs logical computations such as visual reset, on, off, crash, etc.

The Visual Fast subroutine is executed 30 times per second. It computes (and interfaces with CIG) the simulator position and attitude data for cockpits A and B and the lead aircraft when in a formation flying mode. Unlike Logic and Slow subroutines, Fast subroutine is not executed by the executive but directly by a 30/second interrupt handler. The handler in turn is invoked at a 30/second rate by a clock

originating in the CIG special-purpose computer that leads the video frame by 10 milliseconds. This lead allows the Fast subroutine to make the position and attitude updates before CIG starts its frame. The direct connection to the interrupt handler was necessary because the executive could not support a 30/second rate (15/second is maximum) with a fixed 33.33 millisecond interval as required and shown in figure 1. Extensive modification to the executive and module jump list would have been necessary. The fixed interval was necessary in order to compute an accurate transport delay compensation and lead prediction for the interfaced position and attitude data in the Visual Fast subroutine. While the direct method eliminated the need for executive modification, some special considerations were necessary. The Visual Fast subroutine had to meet the restrictions imposed upon interrupt-connected software elements. Specifically, the Fast subroutine could not use common datapool temporaries and math library subroutines since it could interrupt other executive-connected modules using these elements, thereby changing their state. Consequently, all temporaries and subroutines used in the Fast subroutine were made local. The penalty for this was a minor increase in core overhead of approximately 50 words.

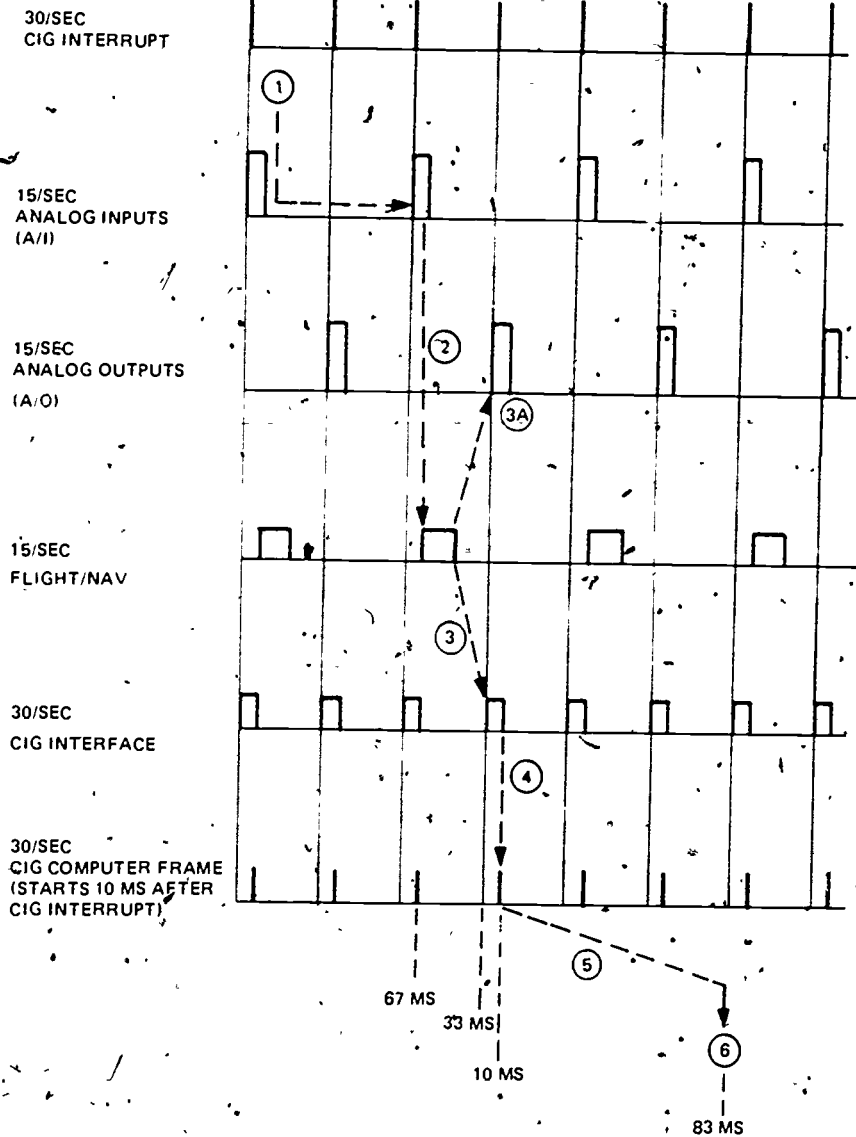
Simulator/CIG Interface Data

Four blocks of fixed-point arithmetic and discrete data are transferred between the simulator and CIG computers. One block is dedicated to cockpit A, one to cockpit B, one to the lead aircraft (cockpit A, B, or the AIOS emulator) when in a formation flying mode, and one block to cockpit A and B miscellaneous discrettes. This data is detailed in tables 1, 2, and 3.

Because of the Interface Control Document (ICD), no addressing, resolution, or definition problems were encountered in interfacing this data.

The method of transferring the data between the basic simulator and CIG was specified to be by means of shared core. Prior to final integration, this method was analyzed and shown to pose a potential problem for the following reasons. Although the CIG computer was required to move the interfaced data to a local (non-shared) area in its own core, no guarantee or protect feature could be designed to safeguard against CIG read/write access to any address in the shared 8K area which comprised 80 percent of the simulator datapool. (Minimum shared core in the SEL 86 system is on 8K word boundaries.)

Therefore, it was possible for the CIG system to overwrite simulator variables, resulting in degraded performance or undefined simulator system aborts and CPU halts.



- 1 CONTROL POSITION CHANGE MADE JUST AFTER TRANSFER OF A/I'S TO CORE MEMORY. INFORMATION MUST WAIT FOR THE NEXT TRANSFER.
- 2 INFORMATION TRANSFERRED TO CORE MEMORY, READ BY FLIGHT
- 3 FLIGHT/NAV COMPUTES STATE CHANGES, PASSES NEW INFORMATION TO CIG INTERFACE PROGRAM
- 3A UPDATED INFORMATION AVAILABLE FOR SIMULATOR A/O'S
- 4 CIG INTERFACE PROGRAM COMPUTES NEW VISUAL STATE VARIABLES AND PASSES THEM TO CIG COMPUTER VIA SHARED MEMORY
- 5 CIG SOFTWARE/HARDWARE REQUIRES 83 MS TO PROCESS UPDATED STATE VARIABLES
- 6 RESULTS OF 1 ARE DISPLAYED BY VISUAL CRT'S.

TOTAL DELAY = 193 MILLISECONDS

NOTE BEST CASE OCCURS WHEN 1 ARRIVES AT LINKAGE JUST BEFORE ANALOG INPUTS ARE TRANSFERRED TO CORE MEMORY AND IS 67 MILLISECONDS SHORTER (126 MS).

Figure 1. WORST CASE VISUAL TRANSPORT DELAY

Table 1. SIMULATOR TO CIG ARITHMETIC DATA TRANSFERS FOR A, B, AND LEAD BLOCKS

Arithmetic Parameter	Description	Block 1 Entry	Units	Scaling	Resolution & Accuracy
$\Delta \text{ lat}$	The latitude coordinate of Williams Air Force Base touchdown point will be subtracted from the extrapolated Simulator A viewing point. latitude ($\Delta \text{ lat} = \phi - 33.299699$).	Word 1	Deg	B_{14}	7.4×10^{-9}
$\Delta \text{ long}$	The longitude coordinates of the central meridian (-111.00) will be subtracted from the longitude coordinate of the extrapolated simulated Aircraft A viewing point. West longitudes are negative ($\Delta \text{ long} = \lambda + 111.00$).	Word 2	Deg	B_{14}	7.4×10^{-9}
hvp	Pilot's viewing point altitude above MSL. The simulated Aircraft A center of gravity altitude above MSL will be extrapolated and added to the vertical component of the vector defining the position of the viewing point relative to the center of gravity.	Word 3	Feet	B_{22}	0.002

Table 1. SIMULATOR TO CIG ARITHMETIC DATA TRANSFERS FOR A, B, AND LEAD BLOCKS (Cont)

Arithmetic Parameter	Description	Block 1 Entry	Units	Scaling	Resolution & Accuracy
$\left. \begin{matrix} C(1,1) \\ C(3,1) \\ C(2,2) \\ C(1,3) \\ C(3,3) \end{matrix} \right\} \left. \begin{matrix} C(2,1) \\ C(1,2) \\ C(3,2) \\ C(2,3) \end{matrix} \right\}$	<p>Matrix of the direction cosines relating aircraft axis system to the flat earth axis system for Aircraft A. The direction cosines will include heading correction to true heading to account for transverse mercator meridian convergence. The convergence term will be zero at coordinates lat = N33.299699, long = W111.0.</p>	Words 4-12	non dim	B_1	9×10^{-10}

17
12

Table 2. SIMULATOR TO CIG DISCRETE DATA TRANSFERS FOR A, B, AND LEAD BLOCKS

Discrete Parameter	Description	Block 1 Entry	1/0
Reset.	The simulated aircraft state vector for Aircraft A is being reinitialized.	Word 13 Byte 0	Reset/Normal
Crash	Simulated Aircraft A has experienced a "crash" condition.	Word 13 Byte 1	Crash/Normal

Table 3. CIG TO SIMULATOR DISCRETE DATA TRANSFERS FOR COCKPITS A AND B

<u>Discrete Parameter</u>	<u>Description</u>	<u>Block 4 Entry</u>	<u>I/O</u>
CIG Ready	The CIG is ready to accept updates of simulated Aircraft A state vector following a simulator reset.	Word 1 Byte 0	Ready/Not Ready
Terrain Collision	The altitude of simulated Aircraft A pilot viewing point is less than the terrain elevation.	Word 1 Byte 1	Collision/Normal
CIG Ready	The CIG is ready to accept updates of simulated Aircraft B state vector following a simulator reset.	Word 1 Byte 2	Ready/Not Ready
Terrain Collision	The altitude of simulated Aircraft B pilot viewing point is less than the terrain elevation.	Word 1 Byte 3	Collision/Normal

Another anticipated problem with regard to shared core was memory parity errors. Frequent parity errors occurred during the development of the basic simulator. It therefore followed that increasing demands on an 8K memory module could result in a prohibitive increase in parity errors and exercise downtime.

To prevent these problems, an alternate method of transferring the required data was studied. In this approach, blocked data is exchanged by means of the SEL 86 automatic input output system together with device controllers and data terminals. The above system would be under program control and therefore would have more potential for safeguarding data pool and would decrease the potential for parity errors through elimination of the additional active shared memory. While this was a desirable feature, implementation would have required development and debug of handlers in both the basic and CIG systems and increased hardware complexity with its potential problems. It was therefore decided to implement the shared-core technique despite its potential risks. During integration, very few parity errors occurred and no actual invalid CIG system memory accesses were encountered. In general, the shared-core approach was straightforward, simple to implement, and problem free.

CIG/Simulator Synchronization

To insure that for each data transfer from the simulation computer, the corresponding frame of video was displayed, and to insure accuracy for the numerical transport delay compensation in the visual interface subroutine, frame synchronization between the simulator and CIG was necessary. Since the video frame rate was 30/second, the same as the basic simulator half-frame rate (the basic simulator rate is 15/second), no special sync problems were envisioned other than implementing a technique. Two ideas were studied. The first idea was to allow the two systems to run on independent 30/second clock sources with the simulation computer monitoring and adjusting for drift due to differences in resolution at one-second intervals, and the second idea was to select one system's clock as master with the other system slaved to it. Both methods required cabling to exchange the clock signal via an interrupt. While the first method was feasible, it required additional software to monitor and adjust for drift of two independent clocks and thereby did not guarantee accurate frame-to-frame synchronization unless the monitor executed at the clock rate of 30/second. This monitor would add significant system timing overhead at a 30/second rate in a system already heavily loaded. The second method however did ensure frame-to-frame synchronization, and the interrupt structure in the SEL 86 with its program control capability lent itself to this technique and hence was the employed method. The only software modification necessary was to incorporate a three-instruction interrupt handler to receive and gate the clock to the simulator computer interval timer, which already served as its normal independent clock 30/second source. Thus, to the

simulation software, the synchronization activity was non-interfering and transparent. The three-instruction handler added a small (approximately 2.5 microseconds) timing overhead per interrupt.

The computer image generator, rather than the basic simulator, was selected as the master to relieve CIG of the burden of system synchronization because there was available in the CIG special purpose computer a hardware generated 30/second clock from the same timing network being used to time the three CIG system computers. This also assured a total common system clock resolution. Hardware was required to make the clock externally available. A shielded cable was used to route the signal to the simulation computer (approximately 60 feet). To insure immediate software handling, the clock was connected to the highest available external interrupt (system override) on the simulation computer.

A potential problem existed in using this level. Because the system override is higher in priority than the peripheral device direct memory access transfer interrupts, its active state could interfere with a data transfer sequence on a high speed device (e.g., disc) causing a data lost condition. Consultation with SEL 86 engineers revealed, however, that this problem would only occur if the interrupt was active longer than 8 microseconds. For this reason, no tasks or services other than gating of the interrupt down to the lower level interval timer was designed into the CIG interrupt handler resulting in an execution time of approximately 2.5 microseconds.

Should interrupting the input/output structure have been a problem, the alternative was to use a lower external level. The next available level however was in priority behind all other interrupts in the system. This represented potentially excessive service delays with an inconsistent frame interval during periods of high interrupt activity which is common in a multi-level task orientated operating system with foreground/background capability.

A fallout advantage of using this level also resulted. It was considered necessary to design into the basic support software a method for selecting the simulator clock or the CIG clock. This would allow independent asynchronous operation of the simulator should a maintenance problem develop in the CIG special purpose clock hardware. Special software incorporated into the simulator executive would have been necessary to provide the above service. However, the system override level has a hardware enable/disable feature via a key-operated switch on the SEL 86 console which in effect performed this function. Thus, selection of clock source and the capability of simulator-dependent or independent operation was simply determined by the turn of a key, without the need for additional software.

This ingenious method of system synchronization was not only simple but proved to be problem-free during the course of integration.

TRANSPORT DELAY

Because of the time required by digital computers to perform the logical and mathematical tasks assigned to them, real time digital simulation consists of the instantaneous sampling of pilot activity (flight control positions, switch positions, etc.), computation of the effects of this sampled activity on the simulator state variables, and feedback of the effects of the updated state variables via instrument indicator light, motion, and visual displays. This cycle is repeated at even time intervals whose length is determined by the speed of operations in the computer and the size of the taskload to be performed. The ASUPT system, having a large taskload, cycles at a maximum rate of 15 iterations per second. All computer input-output and flight dynamics programs operate at this rate, while other rates (7.5/second, 3.75/second, and 1/second) are employed by less time critical programs.

An undesirable result of this iterative scheme is that some increment of time (referred to as transport delay time) must pass before the simulator pilot is provided with feedback resulting from his control activities. If the transport delay time is excessive, the pilot must learn not only to anticipate the dynamic response of the aircraft being simulated, but to compensate for the delays involved in presenting that response to him. The impact of transport time delay is dependent upon the control response expected by the pilot, and his ability to judge the presentation of that response. For instance, transport delays in the ASUPT latitude/longitude inertial position computations (originally computed at 7.5 iterations per second) were not a factor for any task except formation flying, where very accurate judgment of translational rates is required. Increasing the inertial position iteration rates to 15 per second resulted in vast improvements in formation flying position control, but had no noticeable impact on other tasks such as approach and landing maneuvers. The greatest impact of transport delay is in the control of aircraft roll position. The T-37 aircraft has low roll inertia coupled with powerful ailerons and light control forces, resulting in roll response which is rapid and positive. Inclusion of a visual system in the simulation provides, with its horizon extending the full width of the pilot's field of view, a far more precise indication of roll response and dynamics than is available from attitude instrumentation.

Under the limitations of computer time loading as reflected by maximum available iteration rates, transport time delay in the ASUPT system has been minimized. Figure 1 graphically demonstrates the worst case visual time delay for primary control (elevator, aileron, rudder) applications. The difference between worst-case and best-case time delay is due to the fact that

the simulator pilot may make control adjustments at any time, but control positions are sampled by the simulator software only at 66.67 millisecond intervals. The 83 milliseconds required by the visual system software/hardware is indicative of the massive amount of computation required to convert the simulator attitude and positional data into a representative visual display.

The exact impact of the 126 to 193 millisecond transport delay upon the ASUPT roll controllability is unknown, as other problems are thought to exist in this area (see section on Attitude Control). General consensus among the personnel involved with the ASUPT visual integration is that these figures should, ideally, be reduced. Such reductions, however, will require faster computational equipment in order to provide faster iteration rates in the simulation computer and to reduce the 83 millisecond delay in the CIG system.

Time Compensation

The visual interface equations employ the Taylor series for $f(t + \Delta t)$ in order to compensate the visual interface arithmetic data for differences between the time for which they are computed and the time at which they will be displayed by the visual system.

The integration scheme used in the ASUPT flight dynamics equations provides results as follows (see figure 2):

- (1) Analog inputs at time (N) are used to compute accelerations at time (N)

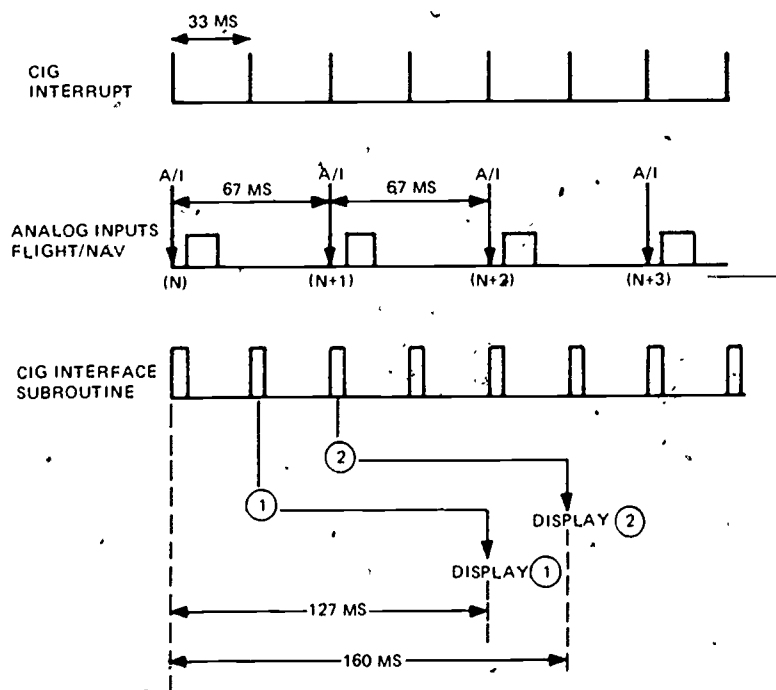


Figure 2. FLIGHT/NAV AND DISPLAY TIMING

(2) Accelerations at (N) are integrated to give velocities at (N+1)

(3) Velocities at (N+1) are integrated to give positions at (N+2)

All of the above parameters and (as a result of the integration formulas) the (N) velocities and (N+1) positions are available to CIG interface cycles labeled ① and ② as shown in figure 2.

The Taylor series is:

$$f(t + \Delta t) = f(t) + \Delta t f'(t) + \frac{\Delta t^2}{2!} f''(t) + \frac{\Delta t^3}{3!} f'''(t) \dots$$

If time (t) is assumed to occur at (N+1):

$$f(t + \Delta t) = f(N+1) + \Delta t f'(N+1) + \frac{\Delta t^2}{2!} f''(N+1) + \frac{\Delta t^3}{3!} f'''(N+1) \dots$$

where Δt is, so far, undefined.

Since $f''(N+1)$, the acceleration at time (N+1), and all higher-order derivatives are unknown during CIG cycles ① and ②, only the first two terms may be used.

$$f(t + \Delta t) = f(N+1) + \Delta t f'(N+1)$$

The value of Δt can be established by reference to figure 2. Time (N+1) occurs 67 milliseconds after time (N), whereas the displays associated with time (N+1) occur 127 milliseconds and 160 milliseconds after time (N):

$$\Delta t \text{ ①} = 126 - 67 = 60 \text{ ms}$$

$$\Delta t \text{ ②} = 160 - 67 = 93 \text{ ms}$$

Time (N+1) has been chosen as the extrapolation basis because of the availability of velocity (N+1); however, this results in the use of a position term which is one iteration behind the latest position term available (N+2). The (N+2) position terms may be used in the following manner.

Assuming:

$$f(N+2) = f(N+1) + 0.067f'(N+1)$$

where 0.067 is the 15 iterations per second quadrature interval.

$$f(N+1) = f(N+2) = 0.067f'(N+1)$$

Then:

$$f(t + \Delta t) = \left[f(N+2) = 0.067f'(N+1) \right] + \Delta t f'(N+1) \\ = f(N+2) + (\Delta t - 0.067)f'(N+1)$$

Resulting only in new set of Δt 's.

$$f(t + \Delta t) = f(N+2) + \Delta t f'(N+1)$$

where:

$$\Delta t \textcircled{1} = -7 \text{ ms}$$

$$\Delta t \textcircled{2} = 26 \text{ ms}$$

This format is used for the lead block data, all translational terms and, originally, cockpit A and B attitude terms.

When problems were encountered in attitude control, the $f''(N+1)$ term was added to cockpit A and B attitude computations in the following manner ($f''(N+1)$ is not normally available).

Assuming:

$$f''(N+1) = f''(N) + 0.067f'''(N)$$

where 0.067 is the simulator quadrature interval.

Then:

$$f'''(N) = \left[f''(N+1) - f''(N) \right] / 0.067$$

By the Taylor series for $f'(N+1)$:

$$f'(N+1) = f'(N) + 0.067f''(N) + \frac{(0.067)^2}{2} f'''(N) \dots$$

$$f'(N+1) = f'(N) + 0.067f''(N) + \frac{(0.067)^2}{3} \left[\frac{f''(N+1) - f''(N)}{0.067} \right]$$

Solving for $f''(N+1)$:

$$f''(N+1) = \frac{2}{0.067} \left[f'(N+1) - f'(N) \right] - f''(N)$$

Adding the third term to the Taylor series, as previously employed:

$$f(t + \Delta t) = f(N+2) + \Delta t f'(N+1) + \frac{\Delta t^2}{2!} \left[\frac{.2}{0.067} \left[f'(N+1) - f'(N) \right] - f''(N) \right]$$

which reduces to:

$$f(t + \Delta t) = f(N-2) + f'(N+1) \left[\Delta t \left[1 + \frac{\Delta t}{0.067} \right] \right] - f''(N) \frac{\Delta t^2}{0.067} - f'''(N) \frac{\Delta t^2}{2!}$$

where all terms are available during CIG cycles ① and ②.

Addition of the Taylor series third term resulted in some improvement in smoothness of the visual presentation, but did not markedly increase roll controllability. Significant improvement was noted, however, in ground control as regards the presentation of heading changes, and their coordination with lateral translation. Since other problems are thought to exist in the roll control area, the improvement was considered significant enough to retain this compensation format in all three attitude axes in spite of the added computation time required.

It should be noted that time compensation schemes such as this cannot eliminate the effects of transport delay. Even though the freshest possible information is used in the visual presentation, and extrapolation may be employed to time-compensate this information, no change in the visual scene can occur as a result of control inputs before the transport delay time has elapsed. The ASUPT system includes a fixed Δt term, summed into Δt ① and Δt ②, whose value is adjustable via instructor

input. Attempts to provide more visual lead via this term resulted in an objectionable lack of smoothness in the visual display. Pilot preference, in fact, resulted in a "backwards" extrapolation (negative fixed Δt) for the attitudes. This was, however, predicated on pilot evaluation of roll response and is thought to be affected by the aforementioned roll control problems.

Of significant note is that transport delay and changes in (or lack of) time compensation are perceived by pilots as changes in the dynamics of the simulated vehicle. Transport delay must be minimized and proper compensation schemes utilized in simulators employing visual systems, especially where highly responsive

vehicles are being simulated. Investigations should be carried out to determine the exact effects of transport delay and compensation schemes, and to determine what, if any, methods may be used to minimize the effect of transport delay on the pilot's ability to control the simulator.

Cue Correction

An important consideration in the integration of a visual system is the coordination, in both onset time and form, of visual cues and kinesthetic cues. The ASUPT simulators are equipped with a six-degree-of-freedom motion system and G-seats. The G-seats are capable, via air pressure activated cells mounted under the seat cushion, of slight reorientations of the pilot's body position with respect to the cockpit environment and of applying differential tactile pressures to his thigh, buttocks, and back areas.

These kinesthetic systems experience transport delays in the same manner as discussed for the visual system, but not necessarily of the same magnitude. Variable lead/lag compensation is provided to the kinesthetic systems, but as was found with the visual system, excessive lead degrades system performance.

The problem presented is; given two systems (visual and kinesthetic) whose onset cues will be presented to the pilot at slightly different times, both of which are some Δt 's behind the pilot action initiating them, should each system be independently optimized, or should the faster system be "slowed down" to correspond to the slower system (assuming, of course, that the slower system has already been optimized)? The solution will require further investigation and analysis.

Also of interest is the form of the onset cues. The time compensation equations were found to be of significant value in altering the form of visual onset cues in the ASUPT system. Essentially, in the case of roll; the pilot's visual perception of roll acceleration was altered by employment of a "backwards" extrapolation term in the visual attitude equations. Extensive instructor inputs are provided in the ASUPT system for altering the kinesthetic drive concepts with regard to transfer function poles and gains, cue shaping functions, and cue acceptance or rejection. Further investigation is being carried out concerning the interrelationships between kinesthetic and visual cues and their effects on pilot performance.

FLIGHT

Attitude Control

One of the major problem areas encountered during visual integration was that of attitude control. Neither the nature of the problem nor the attempted solution are unique to the ASUPT system.³ The problem centered on roll. Although there was also a minor, pitch control problem while yaw was problem free.

Pitch- Dynamic pitch response to elevator movement was initially deemed to be excessive by the acceptance test pilots. Although pilot-induced oscillations were generally not encountered, excessive attention to pitch control was required, thereby unrealistically increasing pilot workload. Satisfactory results were obtained by increasing both pitch damping due to pitch rate and pitch damping due to the rate of change of angle of attack.

Of interest is the fact that the simulator displays a very poorly damped phugoid mode (unlike the aircraft). Several attempts, largely centered on dynamic drag modifications, were made to correct this. No successful means was found of achieving good phugoid damping without adversely affecting other simulated areas, and further efforts were terminated when the modifications to short-period pitch damping provided an easily controllable system.

Roll - Lateral control problems were magnified in the visual integration task. These problems are summarized as follows:

- (1) Inadequate aileron power in the low airspeed (landing approach and slow flight) regime.
- (2) Low aileron stick forces in the slow flight regime.
- (3) Inability to dynamically control bank angle, resulting in roll overshoot and pilot induced oscillations.

The first two problems were satisfactorily solved by modifying aileron roll power and aileron hinge moment coefficient in the applicable dynamic pressure ranges.

The third problem however, proved to be far more complex. The aircraft roll axis is characterized by relatively low inertia and relatively high control power. Pilots expect immediate and positive response of the aircraft to control position inputs, with accelerations into and out of steady roll rates being both rapid and smooth. The problem is further complicated when the

roll axis is being used to control lateral translation in order to establish a ground track (landing approach) or relative position (formation flying).

Initial problems were manifested by the inability to roll the simulator to a desired bank angle without overshoot and subsequent pilot-induced oscillations. Included were pilot comments that control feel was improper, and difficulty was experienced in finding neutral stick position. While the greatest difficulties were observed during formation flight and landing approach, roll control was considered to be unacceptable throughout all flight regimes. Increases were made to aerodynamic roll damping (to improve stability) and aileron roll power (to maintain roll rates). Little could be done during the integration effort with the control stick force feel, since this is largely determined by control loading hardware. Aileron hinge moment per degree of aileron deflection is output from the computer to the hardware at 15/second, but ideally this should be even higher.

Figure 3 depicts stick force/position and a breakout force function deemed desirable. This involved considerable hardware redesign, and therefore, such a function was not possible. Instead, a "deadband" function was placed in the stick position versus aileron deflection computation (see figure 4).

Both the breakout function and deadband function have the same effect on control stick force versus roll rate; some force is required before any roll acceleration is developed. The two differ, however, in that the breakout function does not allow any control stick movement until the breakout force level has been exceeded, while the deadband function allows small control stick movements with no resulting aileron deflection or roll acceleration, thus improving the odds that when the pilot places the control stick at what he feels is the neutral point, there will be zero aileron deflection.

These changes resulted in a control response and feel satisfactory to the acceptance test pilots. Problems arose, however, when pilots not previously exposed to the system were asked to evaluate the simulator. All had difficulty with roll control, especially in finding and holding the wings-level position. This situation phenomenon had been previously encountered. It seems to result from the improvements which had been made in roll control, during basic and visual acceptance, combined with the large amount of simulator flight time accumulated by the acceptance test pilots thereby conditioning them to the simulator. Relatively speaking, the simulator had become much more like the airplane, and the differences in controllability which remained were not felt to be detrimental by the acceptance pilots, who had subconsciously learned to compensate human control functions to overcome deficiencies in the simulator. This occurred in spite of the fact that the acceptance pilots were flying T-37 aircraft as well as the simulator.

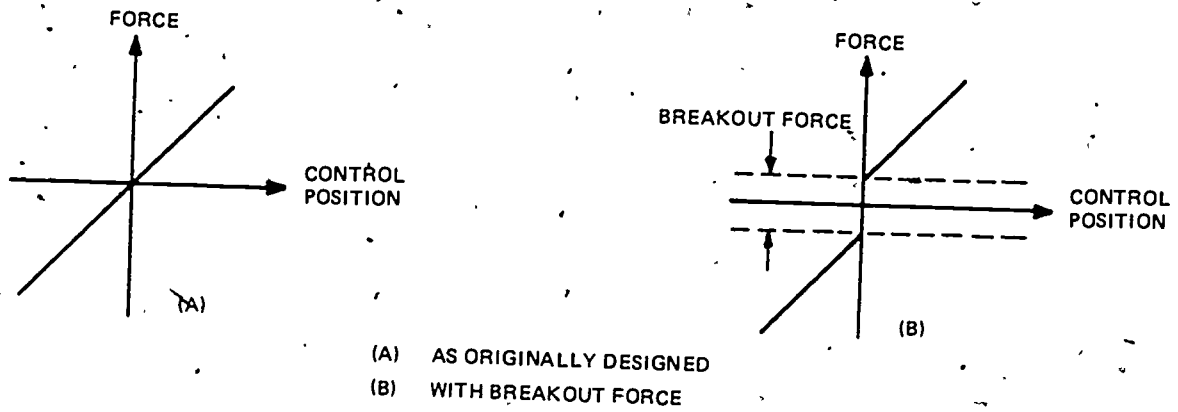


Figure 3. AILERON FORCE VS. CONTROL STICK POSITION

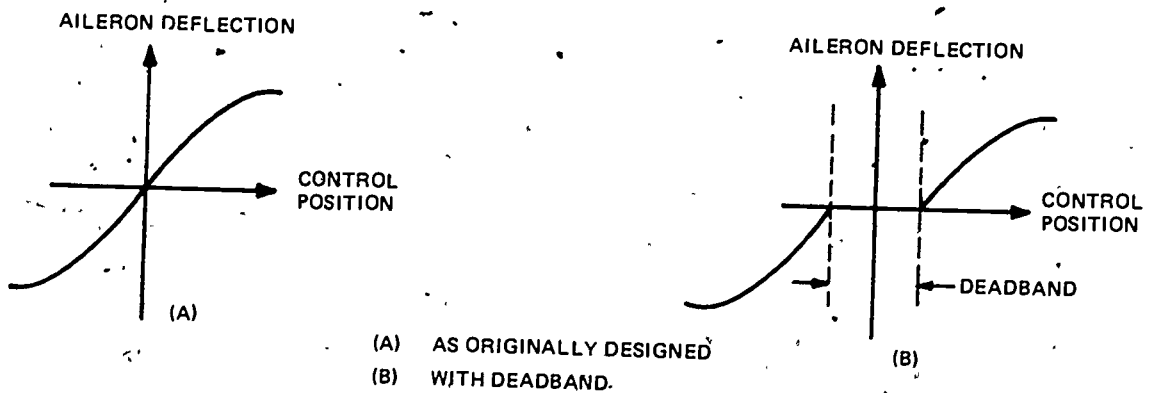


Figure 4. AILERON DEFLECTION VS. CONTROL POSITION

Subsequently, several changes to the simulator software were attempted in a further effort to improve roll controllability. These included modification of the roll and yaw axis aerodynamic coefficients, adjustments to the aileron hinge moment coefficient, and replacement of the control position versus aileron deflection deadband with variously shaped functions. None of these changes were successful.

Further investigations are being performed in the areas of control feel, improved aerodynamic data, and motion effects. A significant limitation may be the visual system transport delay time. Transport delay time may be defined as the time elapsed between a flight control movement and the display of the results of that movement by the visual system. It exists as a consequence of the iterative nature of the simulator computer software and the computer time required by the simulator and visual software/hardware systems to complete the computations required to present a change in the visual scene resulting from control movements. Transport delay in the ASUPT system has been optimized (under the limitations of the simulator computer quadrature interval and visual system delay) to about 126 to 193 milliseconds. The range is due to the sample rate of the simulator's analog input system (15 samples per second given 67 milliseconds between samples). While these times seem short, they are thought to be above the threshold of human perception of the response of a controlled object.

Ground Control

The basic ground reaction equations employed in ASUPT are a relatively complete model in which longitudinal and lateral ground contact forces are computed for each tire, and static and dynamic vertical forces are computed for each strut. These forces are then resolved into aircraft-axes force and moments which are passed to the dynamics equations for summation with the aerodynamic and engine forces and moments. The ground reaction equations are executed at the highest available iteration rate (15 per second in ASUPT).

Simulation fidelity is required in the following areas:

- (1) Taxi
- (2) Takeoff run
- (3) Landing rollout

Required effects to be displayed are:

- (1) Cross wind
- (2) Nosewheel steering

- (3) Rudder steering
- (4) Engine-out effects
- (5) Braking
- (6) Adverse runway conditions (water, ice, etc.)

During the basic simulator acceptance (without the visual system), considerable effort was directed toward ground control evaluation using the compass system and the turn and slip indicators to monitor simulator response. Such efforts, however, are severely handicapped when no "outside world" visual cues are available. In particular, the ability to maintain a desired ground track (for instance, the runway centerline) cannot be evaluated.

Initial evaluation of ground control with the visual system resulted in the following major problem areas:

(1) The simulator was found to be slow to respond to steering inputs (nosewheel, rudder, and differential braking). Considerable amounts of pilot lead were required to obtain and maintain a particular heading.

(2) The simulator appeared to skid whenever heading changes were made. Not only were heading changes required to generate lateral ground track movement excessive, but the lateral movement lagged the heading and required even greater pilot lead to maintain desired ground track.

These problems led to an examination of the nosewheel steering/castering equations and to an examination of the tire side force generation equations.

The T-37 nosewheel steering is activated by depressing a switch on the control stick, which allows nosewheel angle to be controlled via the rudder pedals. When nosewheel steering is not engaged, the nosewheel is free to caster.

The following nosewheel steering dynamic model had been installed during the basic (non-visual) acceptance:

The nosewheel moving away from centered position:

$$\lambda_n = \frac{\lambda_n \text{ demanded}}{0.533s + 1}$$

For nosewheel moving toward centered position:

$$\lambda_n = \frac{\lambda_n \text{ demanded}}{1.361s + 1}$$

During visual integration, the following steering model was incorporated for all steering inputs in order to speed up the response of nosewheel angle:

$$\lambda_n = \frac{\lambda_n \text{ demanded}}{0.0785S + 1}$$

In addition, the location of the nosewheel steering programs was moved from after to just before the ground reaction equations, thus eliminating a one-iteration delay between generation of nosewheel angle and its use in the ground forces and moments computations.

The nosewheel castering model simply sets the nosewheel angle equal to the angle whose tangent is the side velocity of the nose strut divided by the nose strut longitudinal velocity. Essentially, the nosewheel is turned to align it with the direction in which the tire is traveling. The only change made in this area was to "wash out" the castering rate as the forward velocity of the tire goes to zero.

The original side force simulation was as follows:

$$F_{Y_{L \text{ or } R}} = \left[0.76 \left[0.05\psi_{L \text{ or } R} \right]^{LIM \pm 1.0} F_{Z_{L \text{ or } R}} \right]^{LIM \pm \mu_{skid}} \cdot F_{Z_{L \text{ or } R}}$$

$$F_{Y_N} = \left[0.78 \left[0.075\psi_N \right]^{LIM \pm 1} F_{Z_N} \right]^{LIM \pm \mu_{skid}} \cdot F_{Z_N}$$

where: $F_{Y_{L \text{ or } R}}$ = left or right main tire side force, LB

F_{Y_N} = nose tire side force, LB

$\psi_{L \text{ or } R}$ = left or right main tire slip angle, DEG

ψ_N = nose tire slip angle, DEG

μ_{skid} = skid friction coefficient

$F_{Z_{L \text{ or } R}}$ = left or right main strut vertical force, LB

F_{Z_N} = nose strut vertical force, LB

$$\text{and } \psi_{L \text{ or } R} = \tan^{-1} \left[\frac{v_{tL \text{ or } R}}{U_{tL \text{ or } R}} \right] \text{ DEG}$$

$$\psi_N = \tan^{-1} \left[\frac{v_{tN}}{U_{tN}} \right] \text{ DEG}$$

$v_{tL \text{ or } R}$ = left or right main tire lateral velocity, ft/sec

v_{tN} = nose tire lateral velocity, ft/sec

$U_{tL \text{ or } R}$ = left or right main tire longitudinal velocity, ft/sec

U_{tN} = nose tire longitudinal velocity, ft/sec

For conditions "inside" the limits, the gain factors are:

$$\text{main: } (0.76) (0.05) = 0.038 \frac{(\text{LB-side force})}{(\text{LB-vertical force-degree})}$$

$$= 2.1774 \frac{(\text{LB-side force})}{(\text{LB-vertical force-radian})}$$

$$\text{Nose: } (0.78) (0.075) = 0.0585 \frac{(\text{LB-side force})}{(\text{LB-vertical force-degree})}$$

$$= 3.352 \frac{(\text{LB-side force})}{(\text{LB-vertical force-radian})}$$

In order to improve lateral response to steering inputs, the side force generated per unit of slip angle was increased.

The form of the side force computations was changed to the following:

$$\psi_{\text{tire}} = \frac{v_{\text{tire}}}{u_{\text{tire}}} \quad \text{radians}$$

$$F_{Y_{\text{tire}}} = \left[N_{\text{tire}} \psi_{\text{tire}} \right] \text{LIM} \pm \mu_{\text{skid}} F_{Z_{\text{tire}}} \text{LB}$$

where the "tire" subscript may be left main, right main, or nose, and:

$$N_{\text{tire}} = \text{Cornering Power, } \frac{(\text{LB-side force})}{(\text{Radian})}$$

The arctan calls for ψ were eliminated for computer time optimization purposes, and small angle approximation for ψ in radians was employed.

The cornering power curves shown in figures 5 and 6 were approximated from equations given in NASA Technical Report R-644 and were scaled down by the ratios of time vertical force at maximum gross weight.

$$N_{\text{NOSE}} = \left[5.55 F_{Z_N} \right]^{\geq -3640} + 2 \left[-902 - F_{Z_N} \right]^{\geq 0}$$

$$N_{L \text{ or } R} = \left[8.65 F_{Z_{L \text{ or } R}} \right]^{\geq -21,475} + 4.76 \left[-3410 - F_{Z_{L \text{ or } R}} \right]^{\geq 0}$$

(F_{Z_N} , $F_{Z_{L \text{ or } R}}$, N_N , $N_{L \text{ or } R}$ are negative numbers.)

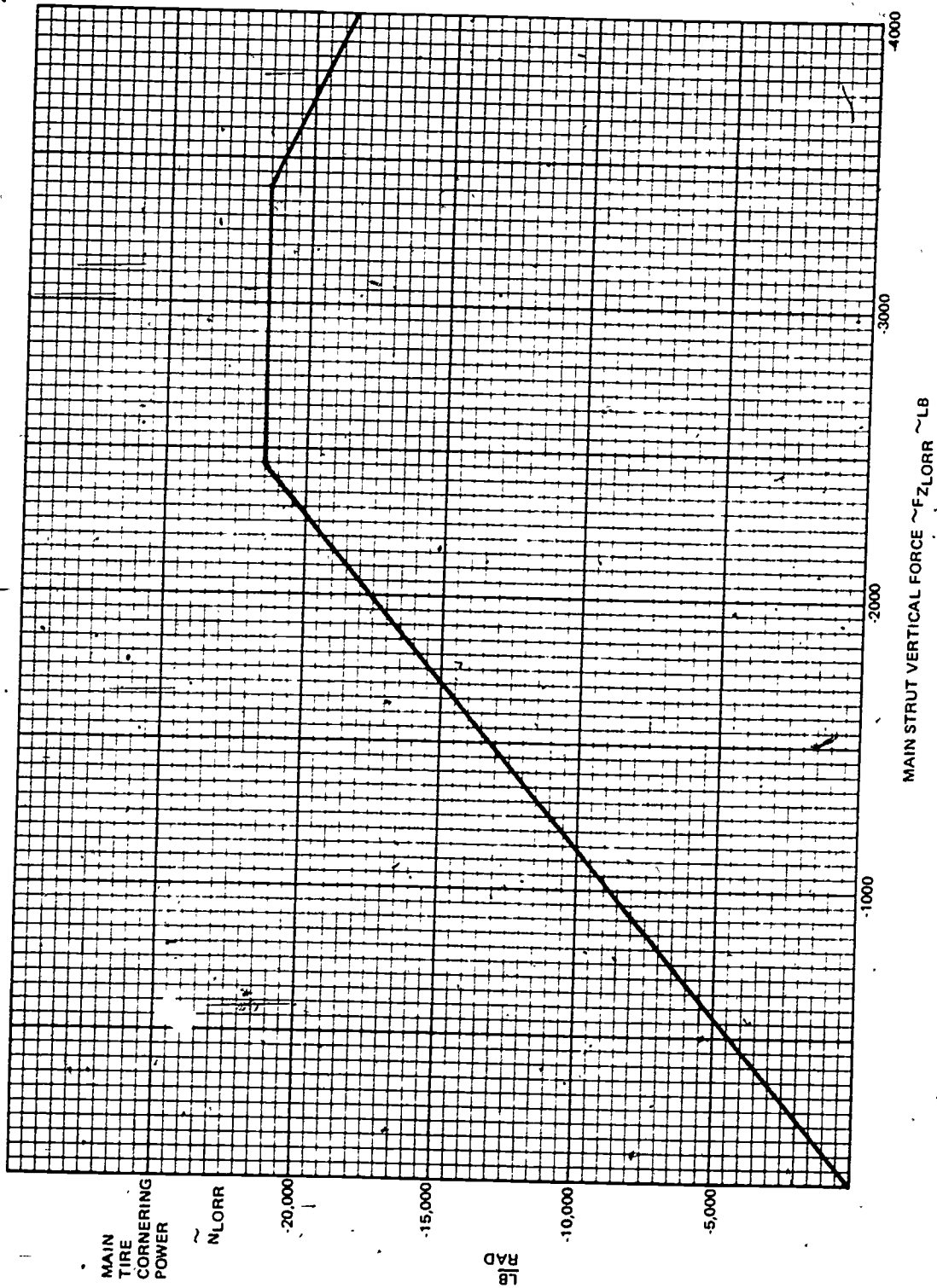
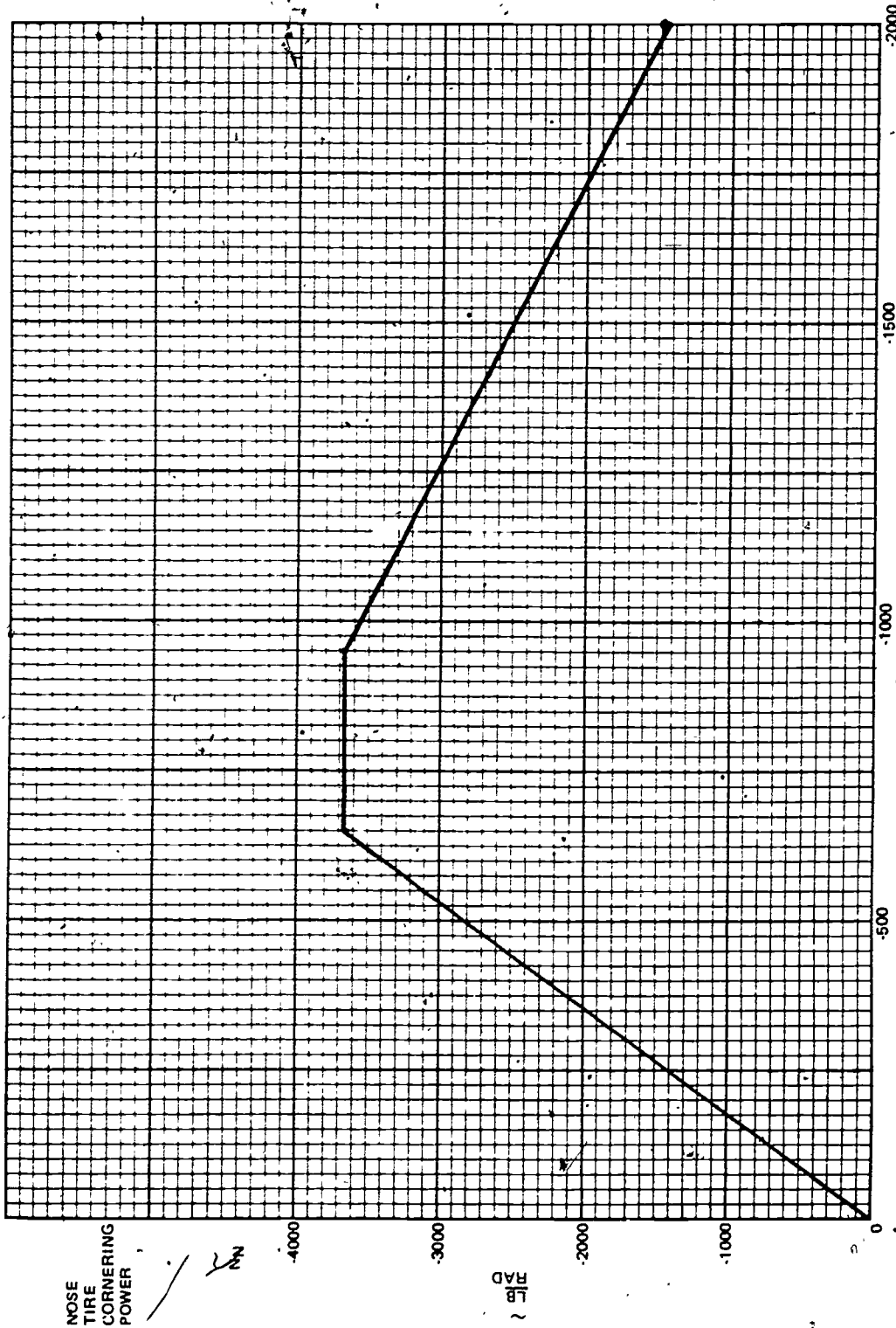


Figure 5. MAIN TIRE CORNERING POWER VS. MAIN STRUT VERTICAL FORCE



NOSE STRUT VERTICAL FORCE ~ FZN ~ LB

Figure 6. NOSE TIRE CORNERING POWER VS. NOSE STRUT VERTICAL FORCE

Note that for this model the gain factors corresponding to those stated for the original model are:

$$\text{Main: } 8.65 \frac{(\text{LB-side force})}{(\text{LB-vertical force-radian})}$$

$$\text{Nose: } 5.55 \frac{(\text{LB-side force})}{(\text{LB-vertical force-radian})}$$

The more rapid nosewheel steering response combined with higher side force gains solved the problems associated with unrealistic system response lags, and eliminated most of the skidding sensations during ground maneuvers. Enough skidding sensation remained, however, to be deemed unacceptable by the acceptance test pilots even though the simulator was fully controllable without excessive pilot effort.

The source of the remaining skidding sensations seemed to be unchanged. A small amount of miscoordination between heading changes and lateral movement remained. In a further attempt to gain more side force from the tires, a spring term (force proportional to lateral tire casing deflection) was added. Such a term already existed, but was used only at very low forward speeds where the slip angle computation becomes indeterminate.

The format was (for each tire):

$$S_t = \left[K \int v_t dt \text{ LIMIT } \pm 1.0 \right] U_{TWV}$$

v_t = true lateral velocity

$K \gg 1.0$

$$U_{TWV} = \left[1.0 - \frac{|U_g|}{8} \right] \text{ LOWR LIM} = 0.$$

U_g = A/C longitudinal speed with respect to the ground, ft/sec

S_t = lateral casing stretch factor, non-dim.

Note that the U_{TWV} term reduced from a value of 1.0 when forward speed was zero, to zero at a forward speed of 8 ft/sec.

The side force resulting from these terms was:

$$F_Y = k_1 S_t F_{Z_t}$$

which was added to the side force resulting from the slip angle term.

The following modifications were made:

$$U_{TWV} = \frac{10}{[U_g]} \text{LOWER LIM TO } 10.$$

and $S_t = [K \int v'_t dt] \text{ LIM TO } \pm U_{TWV}$.

where: v'_t includes lateral true acceleration lead terms computed from the aircraft lateral deceleration and turn acceleration.

Rather than reducing to zero, the stretch factors now reduce in inverse proportion to forward speed, and remain present throughout the ground speed range. In addition, the rate of side force buildup is increased by the presence of acceleration lead.

Again, the degree of skidding was reduced, but the problem was not totally eliminated.

Finally, the modification which solved the problem was entirely pragmatic. The location of the visual viewpoint with respect to the aircraft center of gravity was moved forward approximately 2 feet. The result of this change is to give greater lateral movement of the viewpoint when the simulated aircraft rotates in yaw about the center of gravity, thus compensating for apparent turn/lateral miscoordination.

Spins.

Because the T-37 aircraft is used to demonstrate spins and to teach spin prevention and recovery, realistic simulation of the complete spin regime is required in the ASUPT simulation system. Simulation of the spin maneuver may be broken down into the following areas and requirements:

(1) Entry (deliberate) - proper coordination of roll, yaw, and pitch angles and rates, and proper transition from oscillatory to stabilized spin.

(2) Free spin (rudder neutralized) - proper attitude, heading rate, and descent rate.

(3) Recovery - most rapid recovery should result only when proper recovery techniques are applied. Improper techniques should result in either no recovery or delayed recovery. Application of individual control deflections, whether or not they are in proper recovery sequence, should result in dynamic effects similar to those of the T-37 aircraft.

In addition, the spin simulation should reflect proper characteristics throughout the range of fuel loadings for which spins are allowed in the T-37 aircraft.

Only two types of deliberate spin entries were considered during the ASUPT evaluation (inverted spin entry was not considered):

(1) Erect: entered from wings-level stall, with pitch angle of 30 degrees or less, by application of full rudder in desired spin direction.

(2) Accelerated: entered from banked stall, with pitch angle between 40 and 50 degrees, by application of full rudder in direction of turn.

At the outset of visual integration, the status of ASUPT spin simulation was as follows:

(1) Spin entry: good

(2) Spin with pro-spin rudder: appeared to be proper, except airspeed indication was too high.

(3) Free spin and recovery: unacceptable, the simulator recovered itself as soon as pro-spin rudder was removed.

Further investigation revealed that the simulator was not actually spinning, but rather was descending in a tight spiral (as long as rudder was applied) around a fairly steeply inclined glide axis. The initial problem was seen to be that of obtaining proper free spin characteristics.

The data contained in Air Force Flight Test Center Technical Report No. 70-9⁵ and T.O. 1T-37B-1⁶, in addition to data provided by the acceptance test pilots, were employed to derive the following stabilized free spin characteristics:

$\phi \cong$ Roll angle \cong 0 deg.

$\theta \cong$ Pitch angle \cong -45 deg.

$$\dot{\phi} = \dot{\theta} = 0 \text{ deg/sec}$$

$$\dot{\psi} = \text{heading rate} \approx 1/3 \text{ turn/sec} \approx 120 \text{ deg/sec}$$

$$V_I = \text{indicated airspeed} \approx 40-50 \text{ knots}$$

$$R/C = \text{rate of climb} \approx -11,000 \text{ ft/min}$$

$$a = \text{angle of attack} \approx 45 \text{ deg}$$

$$\beta = \text{sideslip angle} \approx 2 \text{ to } 4 \text{ deg}$$

The angle of attack of -45 degrees follows from the assumption of vertical descent ($\gamma = \text{flight path angle} = -90 \text{ degrees}$) and:

$$a = \theta - \gamma = -45 - (-90) = 45 \text{ deg.}$$

The rate of climb is derived from the representative altitude loss of 550 ft/turn taken from the Air Force Flight Test Center Technical Report No. 70-93 and T.O. 1T-37B-1⁴.

$$(-550 \text{ ft/turn}) (1/3 \text{ turn/sec}) (60 \text{ sec/min}) = -11,000 \text{ ft/min}$$

The sideslip angle is approximated from the heading rate, descent rate, and location of the spin helix axis with respect to the aircraft center of gravity. The spin helix axis enters the aircraft approximately through the canopy bow intersection and exits through the nose wheel well, giving a distance of about 4 to 6 feet from the axis to the aircraft center of gravity.

$$\sin \beta = \frac{V_a}{V_p} = \frac{R(\dot{\psi}/57.3)}{V_p}$$

$$V_a = \text{lateral velocity of C.G., ft/sec}$$

$$R = 4 \text{ to } 6 \text{ ft.}$$

$$\dot{\psi} = 120 \text{ deg/sec}$$

$$V_p \approx \text{descent rate} = -11,000/60 = -183 \text{ ft/sec}$$

$$\sin \beta \approx 0.0458 \text{ to } 0.0687$$

$$\beta \approx 2.62 \text{ to } 3.93 \text{ degrees}$$

From Euler rates ($\theta = \phi = 0$, $\psi = 120$ deg/sec), the stability axis angular rates (p_s , q_s , r_s) may be computed as:

p_s = stability axis roll rate = 2.1 rad/sec

q_s = stability axis pitch rate = 0 rad/sec

r_s = stability axis yaw rate = 0 rad/sec

Note that the pure Euler axis yaw rate is rotated 90 degrees and becomes pure stability axis roll rate; that is, the aircraft rotation is about the vertically oriented X stability axis.

The problem now becomes one of determining the values of roll, yaw, and side force coefficients due to beta and stability axis roll rate (stability axis turn rate is zero) which will solve to zero at $\alpha = 45^\circ$ for the given beta and roll rate. Due to the assumption of all angular accelerations being zero, and because $q_s = 0$ and I_{xz} is small, inertial coupling is not a

factor in the roll and yaw computations. The yawing moment due to side force applied at a forward center gravity location (26% C.G. was assumed) was included. The process was simplified by using the beta coefficients already existing in the simulator. These coefficients were specified by the airframe manufacturer's high-angle-of-attack data (no high-angle-of-attack data were given for angular rate coefficients).

The results of these computations were values of $C_{l_{ps}}$ and $C_{n_{ps}}$ at angle of attack 45° . The value of $C_{n_{ps}}$ showed a low magnitude but of reversed sign, while $C_{l_{ps}}$ reduced to low mag-

nitude, but maintained its sign. These values were incorporated by straight-lining between the coefficient values previously used at $\alpha = 20^\circ$ and the new coefficient values at $\alpha = 45^\circ$. Because of the manner in which they are programmed in the simulator, it was convenient to maintain the value of $C_{l_{ps}}$ constant

for angles of attack greater than 45° , but to continue the slope of $C_{n_{ps}}$ versus α for angles of attack greater than 45 degrees.

These changes resulted in the simulator entering a "flat" spin of very high heading rate at about -10 degrees pitch and +80 degrees angle of attack. The reason for this was seen when total pitch moment (including inertial coupling effects) was

plotted versus α . Two zero values were obtained. The first, at $\alpha \cong 30^\circ$, had an unstable slope, while the second, at $\alpha \cong 80^\circ$, had a stable slope. The high-angle-of-attack pitch moment coefficient was then recomputed in order to move the lower-angle-of-attack zero point from $\alpha = 30^\circ$ to $\alpha = 45^\circ$. While the simulator would still not stabilize at $\alpha = 45^\circ$, it could be "flown" at that angle of attack by judicious use of elevator control, and the validity of the lateral-directional coefficient changes was verified for $\alpha = 45^\circ$.

Attempts to modify the pitch moment slope at $\alpha = 45^\circ$ by tailoring the high-angle-of-attack basic pitching moment coefficient (C_m vs. α), resulted in curves which were obviously unreal, and therefore not programmed. Success was obtained by tailoring $C_{l_{ps}}$ (roll damping coefficient), thus controlling pitch attitude

through the very powerful aircraft axis roll and yaw rate inertial coupling into pitch acceleration. The technique was to reduce $C_{l_{ps}}$ to near zero at $\alpha = 40^\circ$, increase it to the computed

"trim" value at $\alpha = 45^\circ$, then increase the damping sharply above 45 degrees. Thus, as α tends to reduce from 45 degrees, stability axis roll damping reduces and stability axis roll rate increases. This results in an increase in both aircraft axis roll and turn rates, causing a pitch-up moment through the inertial coupling in the pitch acceleration equation, and α is driven back up toward 45 degrees. For α tending to increase above 45 degrees, the opposite takes place. The stability axis roll damping increases, thus reducing the stability axis roll rate, and aircraft axis roll and turn rates. The amount of inertial coupling pitch-up is reduced, and α is driven back down toward 45 degrees.

While these changes solved the free spin problem, they did not provide good recovery characteristics and had adverse effects on entry characteristics.

The T-37 spin entry consists of combined pitch down and roll/yaw in the direction of applied rudder such that the pitch angle (θ) passes through minus 90 degrees with bank angle (ϕ) at or near the inverted position as $\theta = -90^\circ$ is approached. The pitch angle then rises to about horizon level with roll angle at about zero degrees; followed by several pitch/roll and yaw rate oscillations of decreasing magnitude until the stabilized spin is established after three to five turns. The erect entry rates are somewhat higher than the accelerated entry rates, but in neither case does the motion appear (visually) to be violent. Rudder is normally released as soon as the establishment of a spin is verified, but pro-spin rudder (with full aft stick) has only relatively small effects on heading rates and attitude. The stick is maintained in the full aft position until recovery.

Recovery is achieved by application of full anti-spin rudder and, one turn later, full forward stick. The rudder is held until rotation ceases, and the stick is held until the aircraft flies out of the stalled condition in an approximately vertical (or past vertical) dive. All recovery control applications are rapid.

At entry, the simulator tended to snap-roll into the spin; then displayed violent roll, yaw, and pitch oscillations as long as pro-spin rudder was held. When the rudder was neutralized, the oscillations took eight to ten turns to reduce to small ($\pm 5^\circ$) ϕ and θ excursions. Upon application of anti-spin rudder, recovery was immediate and full forward stick was not required.

The violent entry was corrected by adjusting the roll and yaw beta coefficients. The original simulation of C_{l_β} (roll due to beta), expressed as a function of angle of attack, contained a slope change at $\alpha = 8^\circ$, which resulted in very large magnitudes of C_{l_β} at high angles of attack (40 to 50 degrees). This change in slope was removed thus reducing the magnitude of C_{l_β} by a factor of about three in the spin angle of attack region. The C_{n_β} simulation contained a term, commencing at $\alpha = 11^\circ$ and increasing in magnitude proportionately to α above 11 degrees, which caused C_{n_β} to become nonlinear with respect to beta and divergent for large betas. This was also removed, and the low-angle-of-attack slope of C_{n_β} versus α was maintained in the high-angle-of-attack region. The effect of these changes was most apparent in the spin entry, where sideslip angles as high as 20 degrees were generated by rudder application. Changing C_{n_β} changed (slightly) the sideslip angles obtained to about 16 to 18 degrees, while the C_{l_β} change greatly reduced the roll resulting from that sideslip, thus slowing down and smoothing out spin entry. Little effect was noted in the free spin, due to the much smaller sideslip angles and the overwhelming effects of the previously mentioned roll/yaw due to roll rate coefficient changes. The recovery characteristics were improved somewhat (that is, recovery became slightly slower) due to the reduced effectiveness of sideslip angle changes induced by rudder applications, but the simulator would still recover in less than one turn with rudder alone.

This problem was approached via adjustments to the high-angle-of-attack roll, yaw, and side force coefficients due to rudder deflection. The airframe manufacturer's data specifies values for these coefficients at angles of attack of minus 4 degrees and plus 8 degrees. The original simulation consisted of straight-lined functions connecting these data points and continuing,

with constant slope, into the higher angles of attack. The yaw moment and side force coefficients display slopes of increasing magnitude with increasing angle of attack, while the roll moment coefficient has a relatively steep slope of decreasing magnitude, resulting in a reversal of sense and large magnitudes of roll due to rudder in the same direction as rudder deflection in the spin angle of attack region. All three rudder coefficients provided strong recovery tendencies, with the roll coefficient being predominant. Multipliers were developed which reduced the magnitude of each term as a function of angle of attack above 35 degrees. A great deal of experimentation was required to establish multiplier functions which would provide proper recovery characteristics while having minimum impact upon entry characteristics. The final functions resulted in the following rudder only recovery characteristics:

<u>Fuel Weight</u>	<u>Turns to Recovery (Rudder Only)</u>
600 lb	1 to 1.5
1400 lb	4 to 6

The efforts to maintain entry characteristics while adjusting rudder coefficients to obtain proper recovery characteristics were not entirely successful. While the erect entry was still acceptable; the accelerated entry was deficient in both nose-down pitch and roll-off. In addition, acceptance pilots had noted that the power-off and power-on stalls no longer displayed sufficient nose-down pitch.

More roll-off during spin entry was obtained by increasing roll due to turn rate ($C_{l_{rs}}$) as a function of angle of attack above 30 degrees. Also, investigation showed that spin entries were improved as the high-angle-of-attack basic pitch moment coefficient was made more negative in the 16- to 40-degree angle of attack range. The limitation here was nose-up elevator power and inertial pitch effects available to drive angle of attack into the spin region. It was very easy to make c_m negative enough to prevent spin by never allowing angle of attack to reach the 40- to 50-degree range.

Basic pitch moment was then readjusted with the 16- to 25-degree angle of attack values determined by pilot evaluation of stall pitch over characteristics, the 25 to 40 degree values determined by spin entry characteristics and the 45 degree value as determined previously for free spin pitch trim.

Figure 7 traces the evolution of high-angle-of-attack basic pitch coefficient.

During these final phases of spin work, the acceptance (pilots reported several instances of inconsistent entries and recoveries, including failure to enter a spin, rapid recovery, and failure to recover.) A complaint was also received that the "B" cockpit would not spin to the left or recover from a right spin. The latter problem was corrected by maintenance. (The "B" cockpit left rudder pedal forward pedal stop had been mis-adjusted.) The former problem was noted in both cockpits and proved to be more difficult.

Investigation revealed that extremely large magnitudes of roll due to aileron deflection ($C_{l\zeta_a}$) were present at high angles of attack. This coefficient had been developed in the same manner as the rudder coefficients, and had a very large increase in magnitude with increasing angle of attack. A 90 percent reduction in $C_{l\zeta_a}$ was made in the high-angle-of-attack region, and the problems was solved. The apparent cause had been a tendency for pilots to make small lateral stick movements as full rudder was applied for spin entry or recovery.

Two more changes were made during spin development which, while not necessary to the aerodynamic development of spin motion, are important to the pilot's conception of spin characteristics.

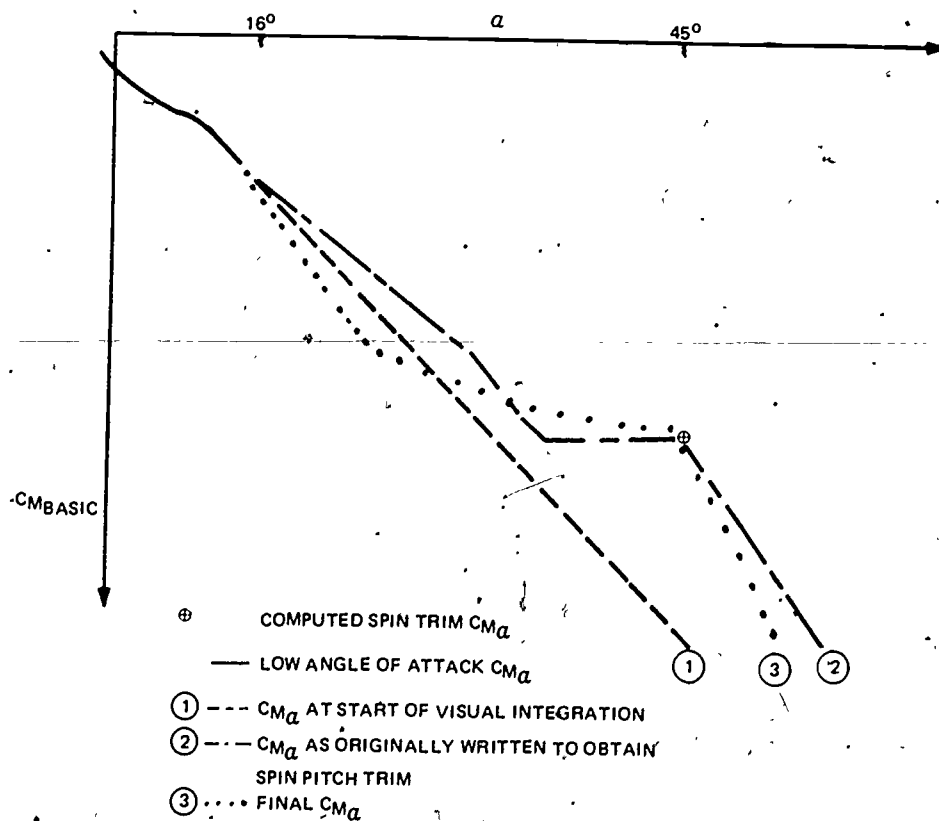


Figure 7. BASIC PITCH COEFFICIENT VS. ANGLE OF ATTACK

The first was to obtain proper airspeed indications at very high angles of attack. The T-37 aircraft indicates 40 to 50 knots of airspeed in the stabilized spin. In the simulation system, the indicated airspeed is derived from the total velocity vector magnitude, which is largely made of an inertial vertical velocity of about 180 feet per second during the spin. In the 15,000 to 20,000 foot altitude range, this converts to an indicated airspeed of about 90 to 100 knots. Since no high-angle-of-attack pitot/static system recovery data was available, a high-angle-of-attack indicator error function was empirically developed to reduce airspeed indications to the proper range.

The second change involved elevator hinge moments. In the aircraft, stick forces become light and the stick moves back against the full-nose-up stop during the spin. High-angle-of-attack functions were added to the elevator hinge moment computations to obtain the desired results.

No claim is made for validity of the aerodynamic coefficients developed during the ASUPT spin evaluations. Obviously, most changes were of a gross nature, made in response to problems as they arose. The only justification is that the results were better than originally expected. While the system is considered to be usable for spin demonstrations and recovery training, some problems are known to exist and some configurations were not investigated. These are as follows:

(1) Attitude - The simulator presently spins at pitch angles between -35 and -40 degrees with angles of attack of about 50 degrees. Both parameters are about 5 degrees nose high.

(2) Stick - No stick buffet is simulated for stall or spin.

(3) Light Fuel Loads - Recovery may be too rapid with fuel loads of less than 800 pounds.

(4) Asymmetric Fuel Loading - The effects of wing fuel imbalance were not investigated.

(5) Inverted Spins - These were not considered.

(6) Nondeliberate Spins - No attempts were made to investigate spin entries from accelerated or deep stalls without the application of rudder.

Formation Flight

The ASUPT Computer Image Generation System contains a selectable data base which consists of a T-37 aircraft and limited ground detail. Extensive shading is employed to present the flat plane surfaces stored in computer memory as curved surfaces in the visual display. Detail level includes insignia, clear canopy with canopy bows, student pilot and instructor heads,

VHF antenna, and flap hinges. The position and attitude of the aircraft model (referred to as lead), is fully adjustable with respect to the ground plane and the simulator (referred to as wing man) pilot's viewpoint. Data for lead attitude and position may come from the opposite cockpit ("A" lead, "B" wing man, or "B" lead, "A" wing man), a time history prestored on the simulator computer's discpack (prestore lead, either "A" or "B" wing man), or a specially constructed emulator system consisting of an attitude control stick and throttle control with simplified equations of motion programmed in the simulator computer's software (Emulator lead, either "A" or "B" wing man). In addition, the effects of the lead aircraft's jet exhaust and wing downwash on the wing man's aircraft are computed and added to the wing man's aerodynamic forces and moments.

Since there are no lower limits on relative separation (in fact, midair collision conditions are computed), a very demanding simulation condition exists: the simulator pilot has very accurate references with which to judge both the attitude and translational performance of the simulator and, unlike the approach to landing situation, these references are available throughout the simulated aircraft's flight regime.

Initially, the acceptance test pilots were unable to smoothly fly in close formation with the lead model, having somewhat greater difficulty when the emulator or prestored "aircraft" was selected as the lead. Problem areas noted were:

- (1) Excessive jetwake/wing wash effects, extending too far behind the lead model.
- (2) Difficulty in judging and controlling closure rates.
- (3) Slow response of the simulator to throttle adjustments.

Since problem area (3), above, was thought possibly to have been a special case of problem area (2) and problem area (2) was obviously related through the control of translational rates via attitude adjustment to the initially experienced attitude control problems, work in these areas was delayed until attitude control improvements could be made.

Wake/wash effects are implemented by computing force and moment increments at (originally) four trailing aircraft wing stations as a function of the relative wind velocity incremental changes created by the lead aircraft's jet exhaust velocity and wing downwash. The position and attitude of the trailing aircraft's wing stations relative to the lead aircraft are computed, and equations for the lead aircraft's jet wake velocity (as a function of engine RPM) and downwash velocity (from vortex theory) are solved at these relative positions and attitudes.

When the effects were reduced, in compliance with pilot comment, it was found that reduction in the number of wing stations considered from four to two did not degrade the simulation, and saved a relatively large amount of valuable computation time (wake/wash effects are computed in a loop, executed once for each station, and involve considerable amounts of computation time in determining relative position and attitude).

The formation flying simulation was again evaluated by the acceptance test pilots after the above wake/wash changes and attitude control improvements had been implemented. The system had improved to the point of being flyable in close formation, but problem areas (2) and (3) were still obvious. Problem (2) was vastly improved by changing iteration rates on both the formation flying computations and the simulator latitude/longitude modules to 15 iterations per second. Originally, these had been computed at 7.5 iterations per second, which was quite sufficient (in the case of latitude/longitude) for all tasks except formation flying (no noticeable improvements in taxiing or take off and landing performance were noted when these changes were made). Acceptance pilots were now able to fly close formation maneuvers smoothly, with the exception of longitudinal positioning: throttle response was still considered poor.

A totally pragmatic solution was to add a small drag function, computed from the difference between demanded engine RPM (throttle position when the engines are fired, windmilling RPM when unfired) and actual engine RPM, thus providing thrust "lead". In addition, the thrust loss due to the thrust attenuators (devices which extend into the engine exhaust stream when speed brakes are extended at near idel engine speeds) was increased. These changes provided the desired longitudinal acceleration control.

When pilots unfamiliar with the simulator evaluated the system (see section on Attitude Control), some difficulty with formation flying was experienced. These problems seemed to be a result of attitude control problems, rather than deficiencies in the formation flying simulation itself. Some difficulty still exists in judging closure rates, but the lack of fine detail (seams, rivets, flight control positions, etc.) on the visual lead aircraft model may be a significant cause.

RECORD/PLAYBACK (R/P)

Incorporated in the basic simulator advanced training software is a system for recording a mission and playing it back. Specifications required that this system be capable of 90 minutes of recording time with fully realistic replay at iteration rates of 1.875 (SLOW), 3.75 (NORMAL), and 7.5 per second (FAST). This system records, on the computer system magnetic tape, critical system (flight, nav/com, and advanced training) discrete and analog inputs such as flight controls, console switches, etc., at

a 3.75/second rate. While NORMAL was the usual replay mode, SLOW could be employed to allow an observer to more closely examine or feel a particular portion of the recording for purposes of evaluation or experimentation. FAST was primarily used to more rapidly position the recording to the area of interest. SLOW was accomplished by halving the module integration rates and slowing the replayed data to 1.875/second, FAST was done by doubling.

In addition to meeting its requirements, this scheme produced a suitable realistic playback via aircraft instruments, controls, and the motion system. This, however, was not the case after integrating the visual with its increased sensitivity. Attitude changes were extremely jumpy and translations had excessive stepping. Therefore, this technique was not acceptable. The cause of this is obvious when considering that the R/P system was recording and replaying only one-fourth of the 15/second flight system control inputs.

— The obvious solution to increasing visual playback fidelity was to record data at faster rates, ideally 15/second. System resources (time and tape space) would not, however, allow a 15/second rate, but could accommodate a 7.5/second rate if the requirement for a total record time of 90 minutes was reduced to 45 minutes. This compromise was made. Software modification was implemented to the R/P system to increase SLOW to 3.75 and NORMAL to 7.5. FAST remained at 7.5, but without doubling the integration constant. Thus, FAST was functionally eliminated (although the hardware controls at the AIOS remained functional). The result was a 50 percent increase in visual playback fidelity with only a noticeable stepping during high-rate maneuvers and rapid flight control activity. Since high rates are encountered in only a minimal portion of the training syllabus, this modification was considered subjectively acceptable. The only negative effect from reducing the total tape record time to 45 minutes was that of maintaining and controlling a larger R/P tape library.

As mentioned above, a NORMAL R/P rate of 15/second would have been the ideal. However, since tape resources (time and space) could not meet this additional load, another larger and faster media, the disc, would have been necessary. Although the basic system was configured with a 24-megabyte disc, it was already dedicated to other system users and spare space would not accommodate the additional R/P requirements. Therefore, this approach was rejected. It would, of course, have been possible to add another disc unit since the system has this expansion capability. This, however, would have required considerably more software modification, together with the cost of additional hardware. Both would have severely impacted the program and the schedule.

SUMMARY

The ASUPT/CIG hardware/software integration effort, which commenced in October of 1974 and was completed in January of 1975, consisted of interfacing the basic simulator computer with the visual system computers, upgrading simulator systems to provide quality dynamic information to the visual system throughout all flight regimes, and total integrated system testing. This report provides a description of the problems encountered during the above integration phases. Each problem is presented in detail together with its solution.

It is apparent that some solutions have not completely resolved the related problems. However, the presentation effects have been minimized to an acceptable level. Such solutions were necessitated by the economics of the situation, where a complete solution would be too costly. One of the purposes of a report such as this is to communicate to others the problems and progress made on such endeavors so that in future undertakings they can address themselves to the problems described herein at an early stage and provide proper and complete solution. This report fulfills that objective.

REFERENCES

1. Larson, D. F. and Terry, C.. ASUPT-76, ASUPT Simulator/Computer Image Generator Integration Acceptance Test Guide, Singer-SPD, Binghamton, N.Y.
2. Hickling, K. ASUPT-59, Interface Control Document ASUPT Simulator/Computer Image Generator Integration. Singer-SPD, Binghamton, N.Y.
3. O'Connor, F.E., Capt. USN; Shinn, Dr. B.J.; Bunker, Dr. W.M. "Prospects, Problems and Performance-A Case Study of the First Pilot Trainer Using CGI Visuals," Document No. 73ASD05, November 1973. General Electric Co., Daytona Beach, Florida.
4. Smiley, Robert F.; Horn, Walter B. "Mechanical Properties of Pneumatic Tires With Special Reference to Modern Aircraft Tires," NASA Technical Report R-64, 1960.
5. Fronter, Maj. Jarry D.; "T-37B Qualitative Spin Tests", Air Force Flight Test Center Technical Report No. 70-9, April 1970.
6. T.O. 1T-37B-1, "USAF Series T-37B Aircraft Flight Manual".

APPENDIX A

ASUPT TECHNICAL FACT SHEET

AIR FORCE



AFHRL/FT TN 73-01

HUMAN RESOURCES

ADVANCED SIMULATION
IN
UNDERGRADUATE PILOT TRAINING
(ASUPT)

TECHNICAL FACT SHEET

By

Frank E. Bell, III

FLYING TRAINING DIVISION
Williams Air Force Base, Arizona 85224

May 1974

LABORATORY

AIR FORCE SYSTEMS COMMAND

BROOKS AIR FORCE BASE, TEXAS

53

48

The Advanced Simulation in Undergraduate Pilot Training (ASUPT) program is a joint effort of two divisions of the Air Force Human Resources Laboratory (AFSC) being conducted under the leadership of the following individuals:

- Hq Air Force Human Resources Laboratory, Brooks AFB, TX

Colonel Harold E. Fischer, Commander
Dr Howard L. Parris, Chief Scientist

- Flying Training Division, Williams AFB, AZ

Lt Colonel Dan D. Fulgham, Chief
Dr William V. Hagin, Technical Director
Mr James F. Smith, Chief, Simulation Applications Branch

- Advanced Systems Division, Wright-Patterson AFB, OH

Dr Gordon A. Eckstrand, Director
Mr Carl F. McNulty, Chief, Simulation Techniques Branch
Mr Don R. Gum, ASUPT Program Manager

This technical summary of the system provides a ready reference to the capabilities of a unique Air Force training research device.



FLYING TRAINING DIVISION
Williams AFB, Arizona

COCKPIT 'A'

ADV IOS

CONV IOS 'A'

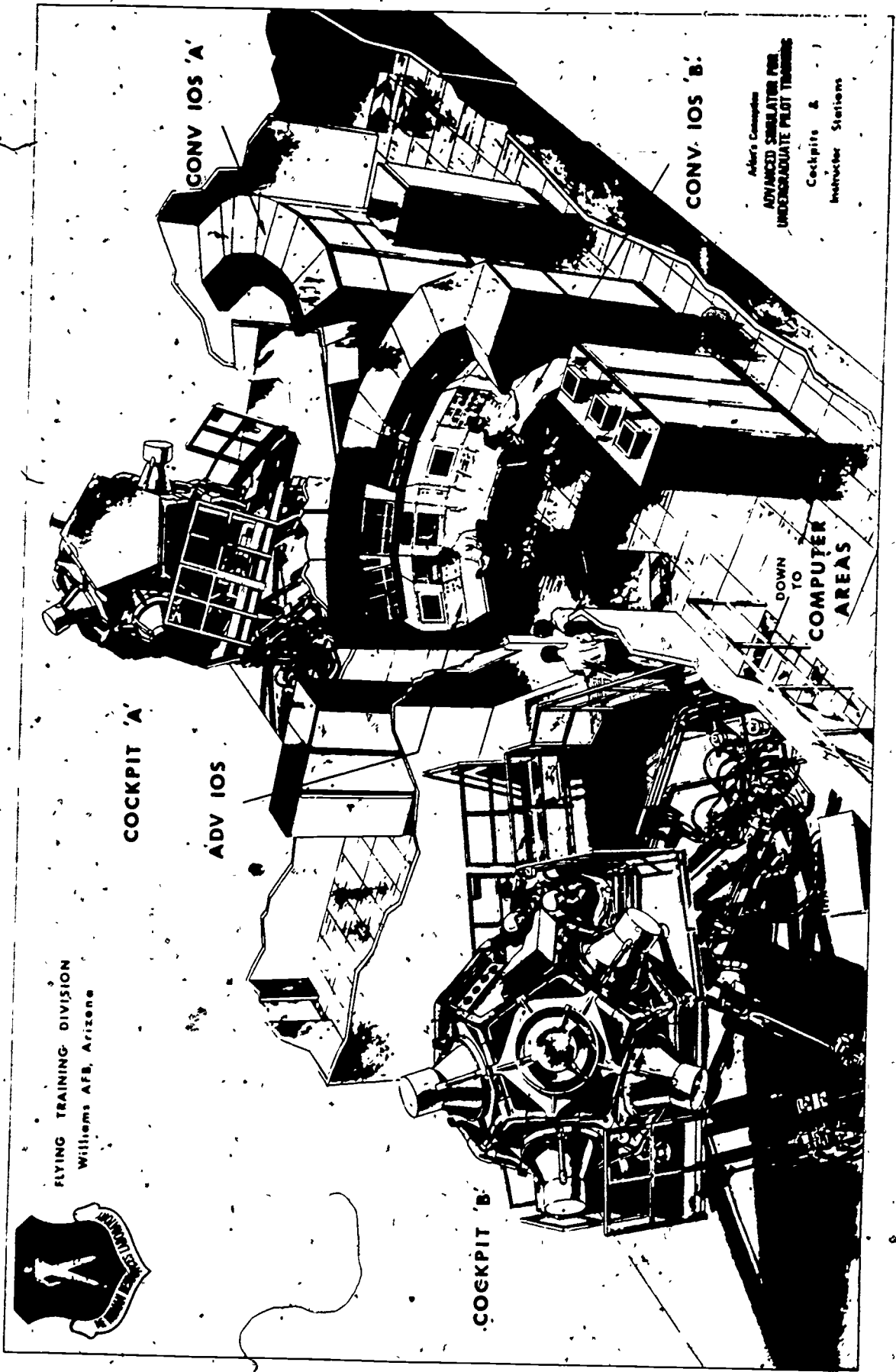
CONV IOS 'B'

Air's Computer
ADVANCED SIMULATOR FOR
UNDERGRADUATE PILOT TRAINING

Cockpits &
Instructor Stations

DOWN
TO
COMPUTER
AREAS

COCKPIT 'B'



ADVANCED SIMULATION IN UNDERGRADUATE PILOT TRAINING (ASUPT)

TECHNICAL FACT SHEET

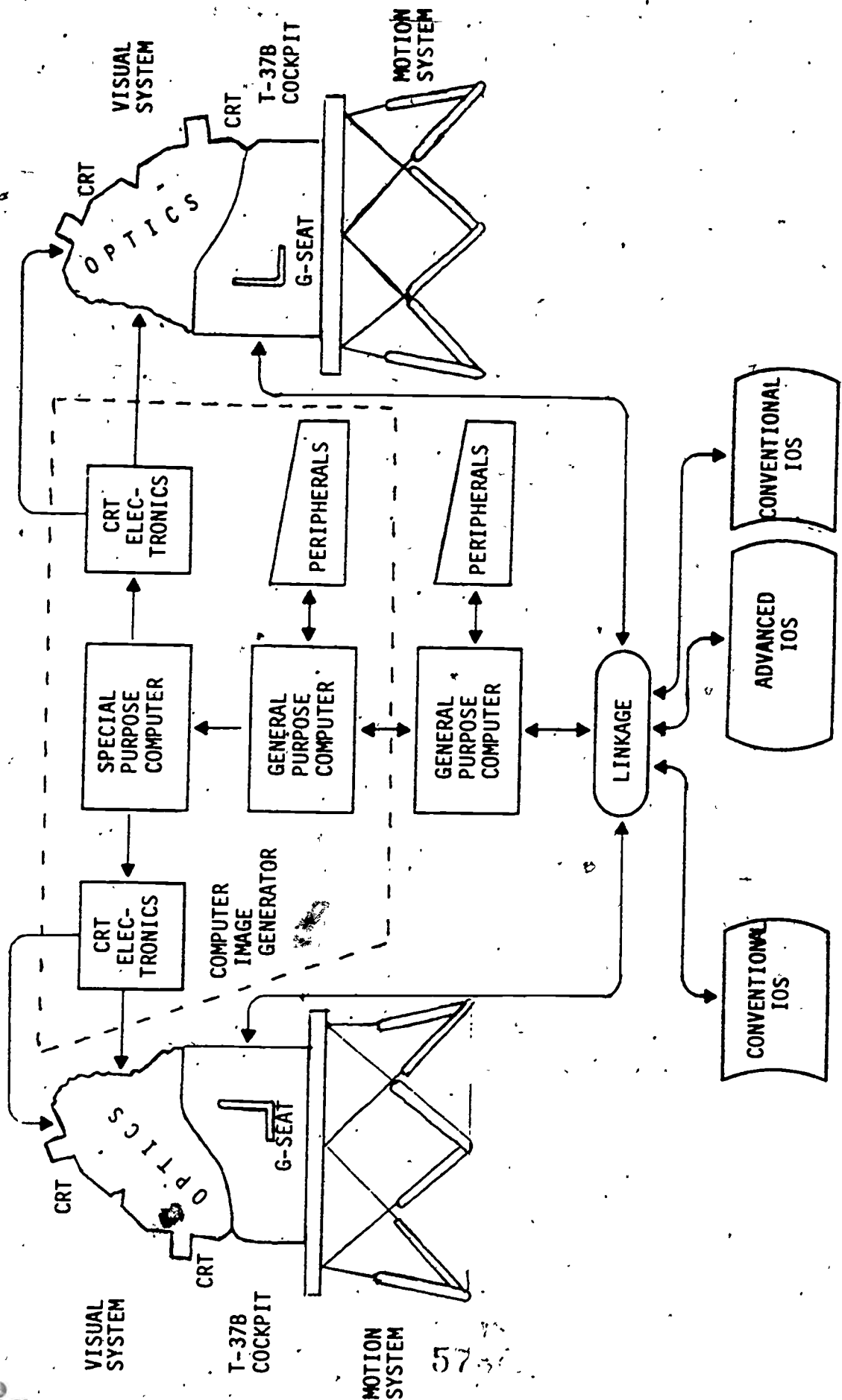
INTRODUCTION

The information in this document has been compiled from a variety of sources and covers only the highlights of the ASUPT system. Readers interested in more technical detail and/or in planned use of the device are referred to the following reports:

1. Taylor, R., et al, "Study to Determine Requirements for Undergraduate Pilot Training Research Simulation System (UPTRSS)", AFHRL-TR-68-11.
2. Juhlin, J. A., et al, "Study to Define the Interface and Options for the ASUPT Visual Simulator", AFHRL-TR-71-47.
3. Gum, D. R., "Development of an Advanced Training Research Simulation System", Proc of the 3d Annual Psychology in the Air Force Symposium, USAFA Department of Life and Behavioral Sciences, April 1972.
4. Hagin, W. V., and Smith, J. F. "Advanced Simulation in Undergraduate Pilot Training (ASUPT) Facility Utilization Plan", AFHRL-TR-74-43.

The major components of the ASUPT system are shown in block-diagram form in Figure 1 and described in subsequent sections. Together they constitute a complex training research vehicle of unlimited potential.

ASUPT BLOCK DIAGRAM



"COMBINED" IOS

FIGURE 1

KINESTHETIC SIMULATION

ONSET CUES

A synergistic six degree-of-freedom motion system has been selected for ASUPT. Each motion platform is driven by six hydraulic actuators and has six passive actuators for safety purposes. The actuators have 60" travel and together provide the following displacement capabilities:

Vertical	+ 38", - 30"	Pitch	+30°, -20°
Lateral	± 48"	Roll	±22°
Longitudinal	+ 49", - 48"	Yaw	±32°

These excursions, in turn, are sufficient for onset cues (with subsequent washout) of the following magnitudes.

Vertical	± 0.8 g	Pitch	± 50°/Sec ²
Lateral	± 0.6 g	Roll	± 50°/Sec ²
Longitudinal	± 0.6 g	Yaw	± 50°/Sec ²

Total Payload: 17,000 lbs

Total Weight on Floor: 26,500 lbs

SUSTAINED CUES

The left-hand (student's) seat in each cockpit consists of 31 pneumatically driven, individually controlled elements:

Seat Pan - sixteen 4" x 4" cells
Back Rest - nine 5" x 7" cells
Thigh Panel - three wedge-shaped cells on the outer side of each thigh.

In addition, the tension in the student's lap belt is varied by a small actuator. By altering the contour of the seat pan and back rest in the "G-seat" and by changing the force exerted by the lap belt, the sustained pressures sensed in the back, buttocks, thighs, and abdomen during flight are simulated.

VISUAL SIMULATION

Each cockpit is virtually enclosed within the seven-channel display subsystem (see Figure 2). Each channel consists of a cathode ray tube (CRT) and a set of in-line optics (Figure 3). The optical components collimate the light rays to provide an infinity image and match the scenes from adjacent CRTs to produce a continuous field-of-view which essentially duplicates that of a T-37 aircraft: $\pm 150^\circ$ horizontally and $+110^\circ$, -40° vertically (Figure 4). The computer generated images appear on the appropriate CRTs, depending on the location and attitude of the aircraft. The ASUPT visual system is unique in that it presents relatively complex scenes in proper perspective over a very large field-of-view during unprogrammed flight paths anywhere within a 500 nautical mile by 500 nautical mile by 100,000 foot airspace.

The CRTs used in the display system are the largest ones in existence, with an overall length of 40" and a chordal diameter of 36". The face-plate is part of a spherical surface 48" in diameter and subtends an 80° angle. Noteworthy features of the tube and its electronics include 1023 scan lines, 1000 elements/line, 30 frames/second, 7 arc-minute resolution, and 600 foot-lamberts highlight brightness. PT462, a high-efficiency, green-tinted phosphor which matches the spectral characteristics of the optics well, is used to produce monochrome scenes.

The passage of images through the optics is illustrated in Figure 5. The polarizers and filters allow the wanted (infinity) image to be transmitted to the pilot while extinguishing the real image and multiple reflections. The path which the wanted image travels results in a significant loss in brightness: the transmission efficiency is approximately 1%. The highlight brightness seen by the pilot, consequently, is 6 ft-lamberts.

The computer image generator (CIG) produces scenes in the following manner. Each object to be displayed is modeled as a set of convex polygonal surfaces. Specifically, the X, Y, and Z coordinates of each vertex of the object are stored on disc along with information associating the vertex with an edge, the edge with a plane polygon, and the polygon with the object. As the aircraft moves through the environment the computer extracts from mass storage only the edge data in the immediate vicinity of its current position. This eliminates processing of data for objects obviously too distant to be seen and allows the number of stored edges to be many times the number of edges actually displayed.

The potentially visible edges are geometrically projected onto seven display planes in order to determine in which channel each is to appear. The intersections of the edges with the scan lines are then computed, priority conflicts resolved, and "gray shades" assigned to the individual raster elements.

The ASUPT CIG is capable of displaying 2000 edges, which may all be used in one simulator or may be shared in any desired ratio between both. For example, if an airwork sortie is underway in cockpit A and traffic pattern practice in B, 500 edges may be processed and displayed for A, 1500 for B. A and B need not be operated within any limited geographic region of the environment model; each is free to fly independently. Special effects such as atmospheric haze and ceilings are incorporated in the system, as are three versions (day, dusk, and night) of the basic model. In addition to fixed objects, the system can display a "moving model" (e.g., another aircraft) for formation or one-on-one training.

The delivered environment model will contain approximately 100,000 edges. The local area of Williams AFB and its auxiliary field, the T-37 contact practice areas, and a 50-mile perimeter around these regions will be modeled with all significant landmarks and features. Surface patterns will occupy the remaining area out to the boundary of the 500 by 500 NM region. Both the simulator and the CIG have been designed for eventual expansion to an area 1250 by 1250 NM. Changes or additions to the model are easy to make for research or training purposes. No other image generation technique shares this flexibility.

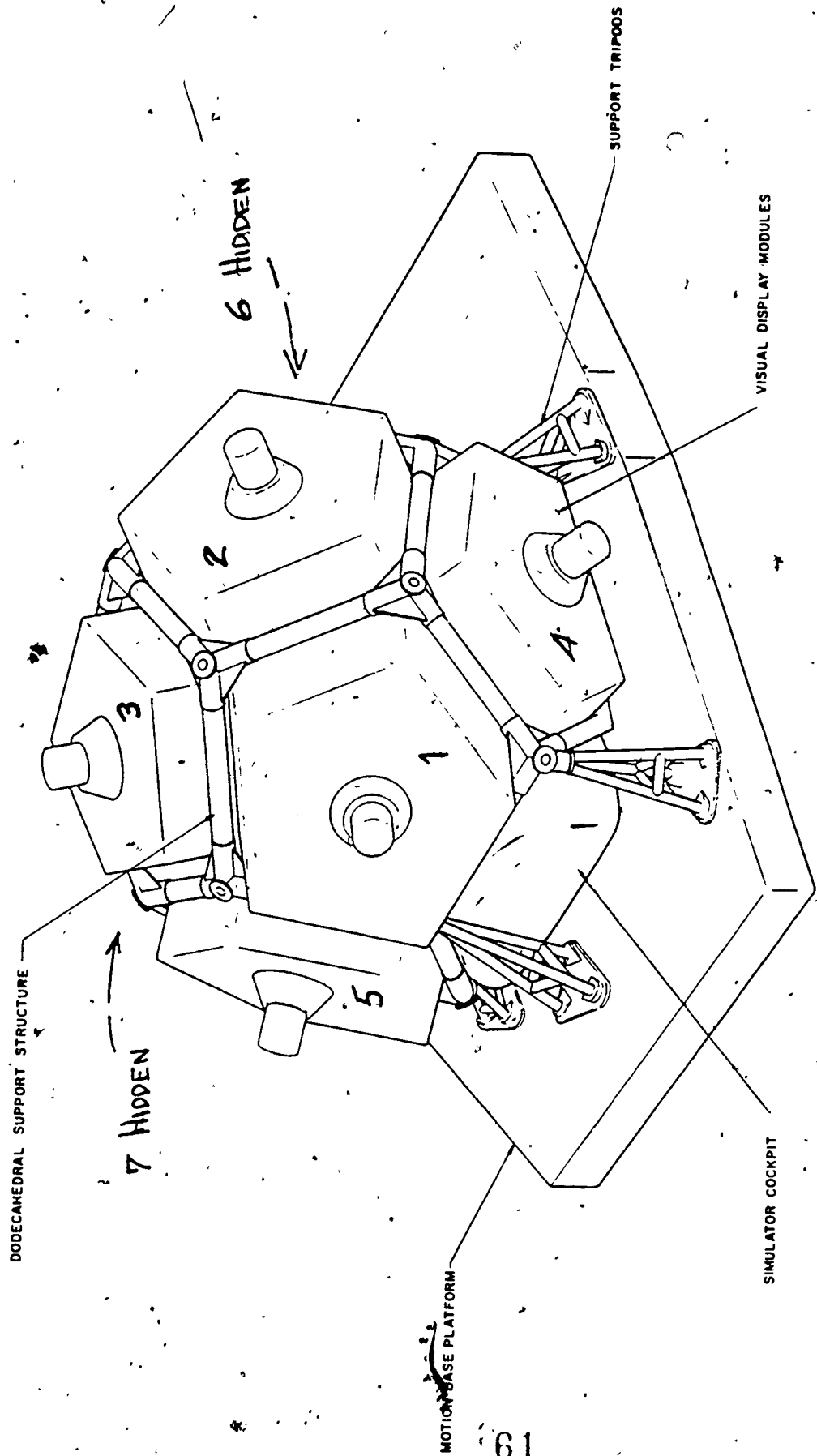


FIGURE 2 VISUAL DISPLAY CONFIGURATION

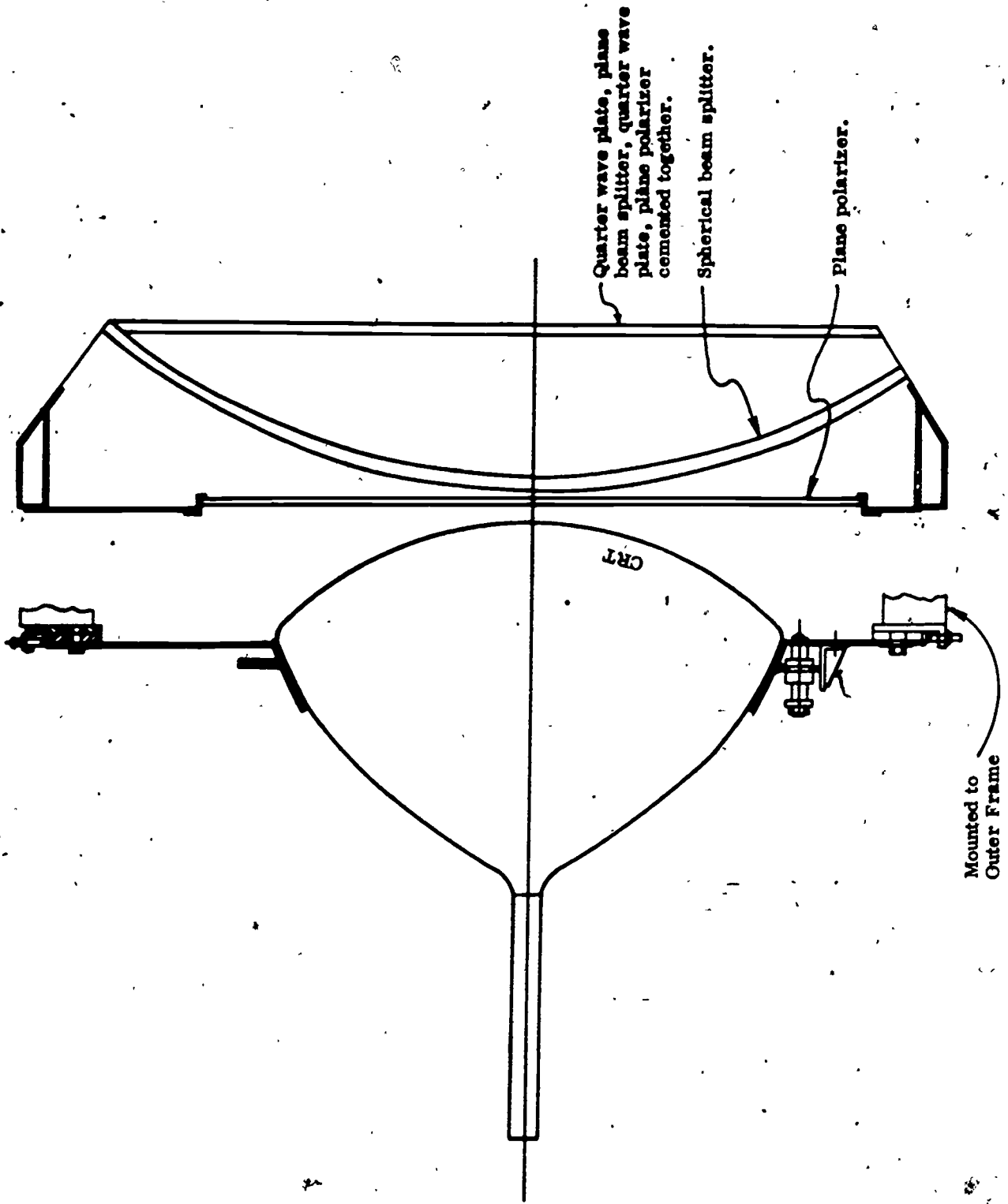


FIGURE 3 Cross Section of Typical Farrand In-Line Infinity Window

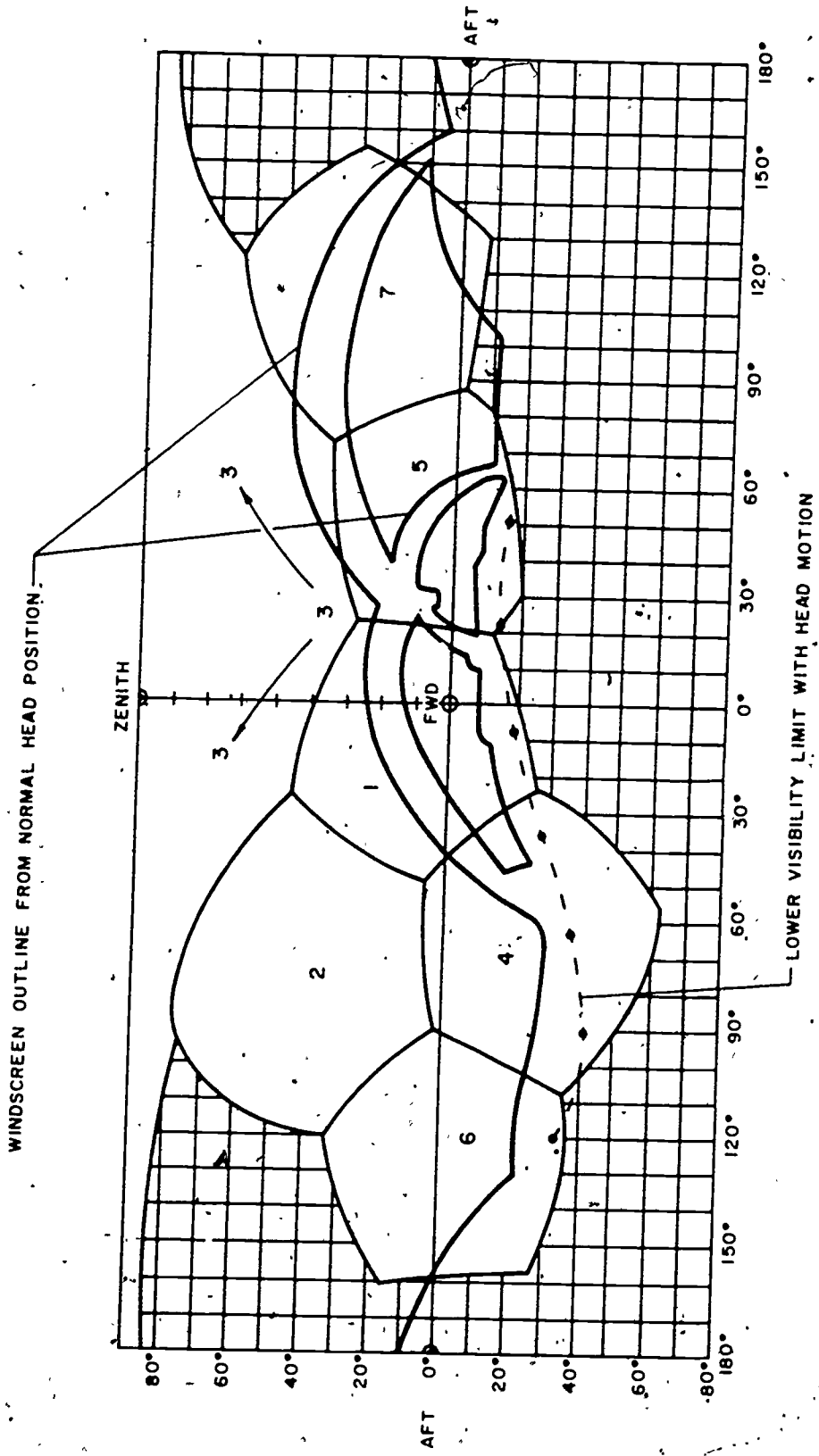
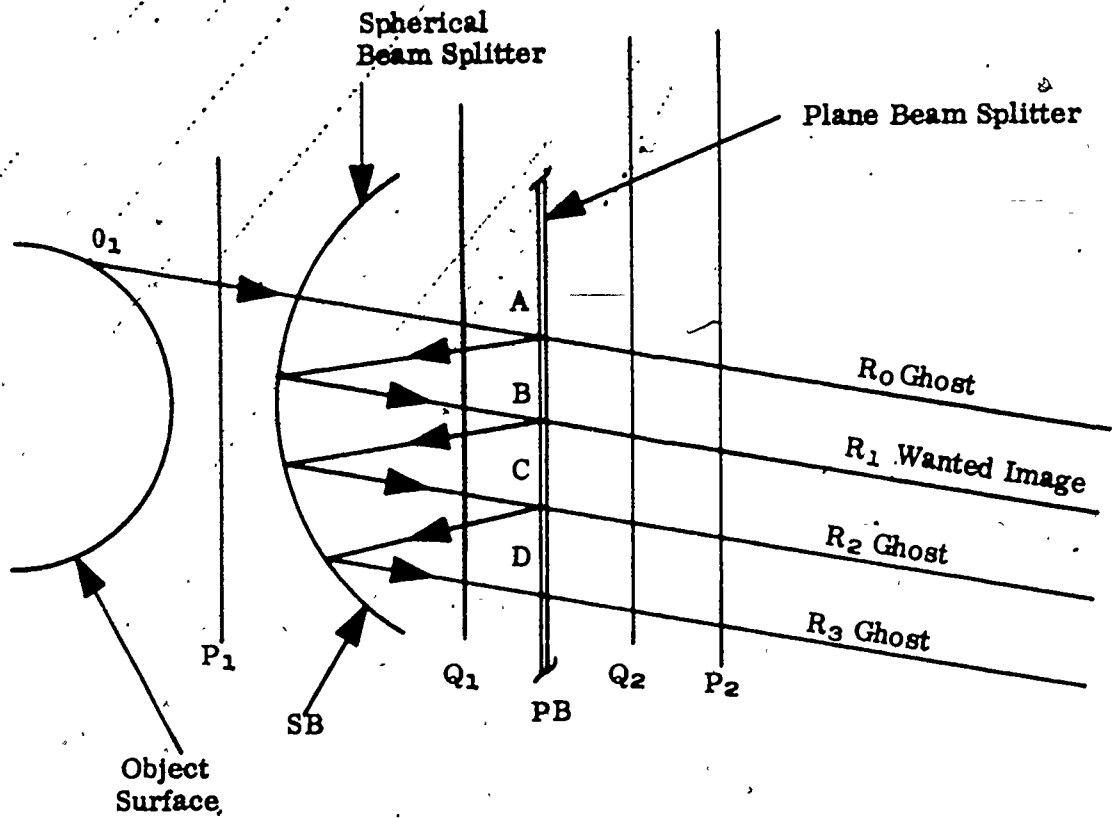


FIGURE 4 VISIBILITY DIAGRAM (PILOT'S POSITION)



P₁, P₂ Plane Polarizers
 Q₁, Q₂ Quarter Wave Plates

FIGURE 5 Schematic Illustration of Farrand Infinity In-Line Optical Display

COMPUTERS & ELECTRONICS

Both the simulator and image generator use the Systems Engineering Laboratories (SEL) Systems 86 general purpose computer, a 32-bit word machine with 600 nanosecond memory cycle speed. Characteristics of the Systems 86 which make it especially well-suited for real-time simulation applications include the following:

Fast instruction execution times (e.g., 1.2 microsecond full word add), which result in a processing speed of 700,000 instructions per second.

Efficient floating point operations only 10% slower than fixed point.

Direct addressing of any bit, byte, halfword, or word anywhere in 128K of memory.

Halfword instructions which can be stored two per memory location.

Very-high-speed I/O channels providing a data transfer rate of 1.67 million words per second.

The general purpose equipment is tabulated below:

ITEM	SIMULATOR (Singer)	IMAGE GENERATOR (General Electric)
Central Processing Units (ea)	1	2
Core Memory (words)	96K	32K
Disc Memory (bytes)	24 Million	16.8 Million
Magnetic Tape Units (ea)	2	1
Line Printers (600 lines per min)	1	1
Card Reader/Punch (200 cards per min read, 100 cards per min punch)	1	1
Teletypewriter (ea)	1	2

The special purpose computer is a hard-wired device which performs the extremely high speed operations necessary to transform the environment data into correct perspective images on all fourteen CRTs every thirtieth of a second. Its sixteen racks include 152,000 32-bit words of dedicated core memory and over 120,000 integrated circuits.

Two independent sets of electronics contain the sweep and function generators, video and deflection amplifiers, and power supplies which drive the CRTs.

INSTRUCTOR/OPERATOR STATIONS

The facility has the capability for control inputs to each simulator from three different types of instructor/operator stations. These stations are referred to as the conventional, in-cockpit, and advanced stations.

The conventional instructor/operator station (CIOS) contains all controls, indicators, displays, recorders, instruments, lights and other equipment necessary to set up, control, and monitor the simulated training mission. The distinguishing feature of the CIOS is that it utilizes repeater cockpit instruments and manual insertion of training conditions similar to existing mission simulators.

The in-cockpit instructor/operator station (ICIOS) is located to the right of the instructor pilot's seat. Its position is such that it may be shielded from the student's sight when the instructor pilot is in the cockpit. The ICIOS console consists of a small CRT display, a keyboard for inputs, and several switches. From this station, the instructor can interact with the computer to call up malfunctions, performance demonstrations, and all other advanced training capabilities. When solo, the student will be able to see the in-cockpit console CRT and may be supplied training information on this display.

The advanced instructor/operator station (AIOS) contains a keyboard, four computer driven CRT's, a stick for providing control inputs to either simulator, and other equipment required to implement the advanced instructor provisions described below. Two of the CRT's display seven color alpha numeric information in a raster scan format. The other two can also provide alpha numeric characteris, but are designed for graphic information such as navigation charts, GCA approaches, and lead and wing aircraft situation display for formation or one-on-one training; these CRT's use a stroke scan format. Any information available at the CIOS can be reformatted and displayed on an AIOS CRT. In addition, virtually any parameter in the computer can be called up for display. For example, a real-time plot of airspeed vs altitude during final approach can be generated and displayed along with a prestored plot of the ideal approach. A hard copy can be produced to use when debriefing the student. Finally, the AIOS is located immediately adjacent to one of the conventional stations to permit the study of potential console designs which contain a mixture of standard and advanced instructional features. In this mode, the console is termed the combined IOS.

At each CIOS are three video monitors, one providing a closed circuit TV picture of the student in the cockpit and the other two displaying selectable channels of his visual scene.

ADVANCED INSTRUCTIONAL FEATURES

The ASUPT research facility has extensive capabilities involving instructional techniques, some of which are not now available in conventional simulators. These capabilities include: selective task sequencing; variable task difficulty and complexity; selective malfunction insertion; freeze; rapid reinitialization; automated demonstration; knowledge of results; and self confrontation. Following is a brief discussion of each of these capabilities.

1. Task Sequencing.

There are four methods of sequencing possible: Instructor Directed Manual (IDM); Student Directed Manual (SDM); Explicit Ordered Automatic (EOA); and Computer Ordered Automatic (COA). In IDM, the instructor pilot (IP) selects the next task depending upon the student's performance, required accomplishments, and in general, the IP's judgment. The SDM mode allows each student to select the tasks in an order satisfactory to himself. This presupposes a knowledge of required elements and their interrelationships, but it has a sound basis in learning technology. EOA permits preprogramming of task sequence prior to a sortie. This mode provides the instructor or experimenter with a fixed task order for a group of students; such an arrangement is mandatory for rigid experimental control. COA is the ultimate approach: the computer selects the sequence based on task importance, difficulty level, student ability and previous performance to provide optimum individual sequencing.

2. Task Difficulty and Complexity. Any given task may have several levels of difficulty and complexity. These variables are dependent on four factors.

a. Degrees of Freedom of Motion. Aircraft motion is a combination of displacements in six dimensions: longitudinal, lateral, vertical, roll, pitch, and yaw movements. Simulated aircraft movement can be restricted to any combination of the six degrees-of-freedom desired.

b. Aerodynamic Response. The simulator allows for variation of aircraft response to control movements. For example, stability could be decreased to increase task difficulty.

c. Malfunction Insertion. The type and number of malfunctions determine task loading and therefore influence overall task complexity and difficulty.

d. Environmental Factors. Wind velocity and direction, temperature, and turbulence affect maneuver difficulty.

3. Malfunction Insertion. The inclusion of malfunctions (simulated emergencies) into training may be accomplished one of three ways:

a. Direct - immediate initiation, performed from any instructor location.

b. Automatic/Explicit - insertion into the mission when a pre-determined set of conditions occur.

c. Automatic/Probabilistic - insertion into the mission as a function of several parameters, one of which is random.

4. Freeze.

The freeze mode is similar to existing simulator capabilities. Its selection by the student, instructor, or experimenter stops the simulator; all instruments and visual displays stop in their position. This capability gives the student time to catch up, lets the instructor's briefing remain current with the aircraft, or lets him emphasize a particular point.

5. Reinitialization.

This is the ability of the system to place the simulated aircraft at a particular point in space and with a given configuration without "flying" it there. For example, in learning the turn to final the student can start from the downwind, fly to touchdown, reinitialize back to the downwind and attempt it again. This permits maximum practice of the prescribed maneuver in the allotted time.

6. Automatic Demonstration.

This capability permits the student, instructor, or experimenter to call for the demonstration of a selected maneuver or a part thereof. "Perfect" maneuvers will be recorded and stored for this use. Playback will involve all motion cues, instrument readings, and visual scenes of the total simulator system. Recorded audio instruction synchronized with the visual display will accompany the playback when desired. Portions of the maneuver can also be selected for maximum flexibility. This

capability allows standardization of maneuvers and instructional techniques. In addition, it permits students to see and then practice, without an instructor present.

7. Knowledge of Results.

Students can be provided knowledge of results (KR) on their performance in several ways. Available techniques include performance playback, CRT presentation, alpha numeric score, audio message, or any combination of these.

8. Self-Confrontation (SC).

SC permits the student to examine his own performance through a playback of that performance using all systems including stick, throttles, and rudder. This playback can be presented in slow, real, or fast time (except motion) for demonstration and KR. Such self-observation enables the student to evaluate his behavior from a more objective position and is expected to lead to large behavior changes in short periods of time.